THE JOURNAL OF BIOLOGICAL CHEMISTRY VOL. 282, NO. 22, pp. 16295–16307, June 1, 2007

Inactivation of the Phosphoinositide Phosphatases Sac1p and Inp54p Leads to Accumulation of Phosphatidylinositol 4,5-Bisphosphate on Vacuole Membranes and Vacuolar Fusion Defects*[S]

Received for publication, February 2, 2007, and in revised form March 28, 2007 Published, JBC Papers in Press, March 28, 2007, DOI 10.1074/jbc.M701038200

Fenny Wiradjaja[‡], Lisa M. Ooms[‡], Sabina Tahirovic[§1], Ellie Kuhne[‡], Rodney J. Devenish[‡], Alan L. Munn[¶], Robert C. Piper[‖], Peter Mayinger[**], and Christina A. Mitchell[‡2]

*From the [‡]Department of Biochemistry and Molecular Biology, Monash University, Clayton 3800, Victoria, Australia, [§]ZMBH, University of Heidelberg, INF 282, 69120 Heidelberg, Germany , the [¶]Institute for Molecular Bioscience, Queensland Bioscience Precinct, University of Queensland, St. Lucia, Queensland 4072, Australia, the [‖]Department of Physiology and Biophysics, University of Iowa, Iowa City, Iowa 52242, and the **Division of Nephrology and Hypertension, Oregon Health and Science University, Portland, Oregon 97239*

Phosphoinositides direct membrane trafficking, facilitating the recruitment of effectors to specific membranes. In yeast phosphatidylinositol 4,5-bisphosphate (PtdIns(4,5)P_2) is proposed to regulate vacuolar fusion; however, in intact cells this phosphoinositide can only be detected at the plasma membrane. In *Saccharomyces cerevisiae* the 5-phosphatase, Inp54p, dephosphorylates PtdIns(4,5)P_2 forming PtdIns(4)P, a substrate for the phosphatase Sac1p, which hydrolyzes (PtdIns(4)P). We investigated the role these phosphatases in regulating PtdIns(4,5)P_2 subcellular distribution. PtdIns(4,5)P_2 bioprobes exhibited loss of plasma membrane localization and instead labeled a subset of fragmented vacuoles in Δ*sac1* Δ*inp54* and *sac1^{ts}* Δ*inp54* mutants. Furthermore, *sac1^{ts}* Δ*inp54* mutants exhibited vacuolar fusion defects, which were rescued by latrunculin A treatment, or by inactivation of Mss4p, a PtdIns(4)P 5-kinase that synthesizes plasma membrane PtdIns(4,5)P_2. Under these conditions PtdIns(4,5)P_2 was not detected on vacuole membranes, and vacuole morphology was normal, indicating vacuolar PtdIns(4,5)P_2 derives from Mss4p-generated plasma membrane PtdIns(4,5)P_2. Δ*sac1* Δ*inp54* mutants exhibited delayed carboxypeptidase Y sorting, cargo-selective secretion defects, and defects in vacuole function. These studies reveal PtdIns(4,5)P_2 hydrolysis by lipid phosphatases governs its spatial distribution, and loss of phosphatase activity may result in PtdIns(4,5)P_2 accumulation on vacuole membranes leading to vacuolar fragmentation/fusion defects.

Phosphoinositide signaling molecules are phosphorylated derivatives of phosphatidylinositol (PtdIns)[3] that play critical roles regulating the actin cytoskeleton, cellular proliferation, and vesicular trafficking (1). PtdIns can be reversibly modified by lipid kinase phosphorylation of the D-3, D-4, or D-5 positions of the inositol head group to create phosphorylated phosphoinositides that recruit and activate effectors containing phosphoinositide-binding domains (1). In yeast and mammalian cells, phosphatidylinositol 4-phosphate (PtdIns(4)P) regulates secretion from the Golgi, and PtdIns(4)P recruitment of specific effector proteins, including FAPP1 and FAPP2, is required for mammalian Golgi to plasma membrane trafficking (1–3). In *Saccharomyces cerevisiae* PtdIns(4)P is synthesized from PtdIns by three PtdIns 4-kinases, Pik1p at the Golgi, Stt4p at the plasma membrane, and Lsb6p at the plasma and vacuolar membrane (4–7). In yeast, phosphatidylinositol 4,5-bisphosphate (PtdIns(4,5)P_2) is generated from PtdIns(4)P by the PtdIns(4)P 5-kinase, Mss4p (8). PtdIns(4,5)P_2 is involved in the regulation of endocytosis, actin cytoskeletal dynamics, and the maintenance of Golgi structural integrity (1).

Phosphorylated phosphoinositides are dephosphorylated by lipid phosphatases that regulate the temporal and spatial distribution of phosphoinositide signals. In yeast, PtdIns(4)P and PtdIns(4,5)P_2 are hydrolyzed by phosphoinositide phosphatases, including Sac1p and the inositol polyphosphate 5-phosphatases (5-phosphatases), Inp51-4p (9–12). Sac1p is a polyphosphoinositide phosphatase containing a CX_5R catalytic motif, which is found in both SacI domain-containing lipid phosphatases, as well as dual specificity tyrosine and serine/threonine phosphatases. Four active SacI domain-containing lipid phos-

* This work was supported by the Australian Research Council Centre of Excellence-Structural and Functional Microbial Genomics Grant CE0562063, Australian Research Council Grant DP0345120 (to C. A. M.), National Health and Medical Research Council Project Grant 298921 (to A. L. M.), and National Institutes of Health Grant GM071569 (to P. M.). The costs of publication of this article were defrayed in part by the payment of page charges. This article must therefore be hereby marked "*advertisement*" in accordance with 18 U.S.C. Section 1734 solely to indicate this fact.

[S] The on-line version of this article (available at http://www.jbc.org) contains supplemental Figs. 1–5.

[1] Present address: Max Planck Institute for Neurobiology, 82152 Martinsried, Germany.

[2] To whom correspondence should be addressed: Dept. of Biochemistry and Molecular Biology, Monash University, Wellington Rd., Victoria 3800, Australia. Tel.: 613-9905-3790; Fax: 613-9905-3726; E-mail: Christina.Mitchell@med.monash.edu.au.

[3] The abbreviations used are: PtdIns, phosphatidylinositol; PtdIns(3)P, phosphatidylinositol 3-phosphate; PtdIns(4)P, phosphatidylinositol 4-phosphate; PtdIns(4,5)P_2, phosphatidylinositol 4,5-bisphosphate; PH-OSBP, pleckstrin-homology domain of oxysterol binding protein; PH-PLC, pleckstrin-homology domain of phospholipase C; PH-Num1p, pleckstrin-homology domain of Num1p; CPY, carboxypeptidase Y; ALP, alkaline phosphatase; vps, vacuolar protein sorting; GFP, green fluorescent protein; ER, endoplasmic reticulum; HPLC, high pressure liquid chromatography; chr, chromosome; PH, pleckstrin homology; OSBP, oxysterol-binding protein; CMAC, 7-amino-4-chloromethylaminocoumarin; V-ATPase, vacuolar ATPase; OCRL, oculocerebrorenal protein of Lowe.

phatases exist in *S. cerevisiae*, including Sac1p, Fig4p, and two of the four 5-phosphatases, Inp52p and Inp53p (also called Sjl2p and Sjl3p) (10, 13). The SacI domain of Inp51p/Sjl1p lacks the CX_5R motif and is therefore catalytically inactive. Sac1p hydrolyzes PtdIns(4)P, PtdIns(3)P, and PtdIns(3,5)P_2 to PtdIns, but PtdIns(4)P is the preferred substrate (10). Sac1p localizes to the endoplasmic reticulum (ER) by interaction with dolichol-phosphate mannose synthase Dpm1p during the exponential phase of cell growth and translocates to the Golgi when nutrients become depleted (14). Sac1p regulates Golgi membrane trafficking by controlling PtdIns(4)P levels (15). The s*ac1* null phenotype is complex, including altered phosphoinositide metabolism, accelerated phosphatidylcholine biosynthesis, cold sensitivity, inositol auxotrophy, hypersensitivity to multiple drugs, actin and cell wall defects, and delayed endocytic and vacuolar trafficking (16–21). Mutations in *SAC1* bypass the requirement for the phosphatidylinositol transfer protein, Sec14p, in regulating protein transport from the Golgi to the plasma membrane (22).

The 5-phosphatases Inp51-4p hydrolyze PtdIns(4,5)P_2 forming PtdIns(4)P via their central 5-phosphatase domain. Single null mutation of any SacI domain-containing 5-phosphatase shows little phenotype; however, *inp51 inp52* and *inp52 inp53* double mutants show overlapping functions/phenotype, including actin cytoskeletal disruption, endocytic defects, abnormal cell wall integrity, and vacuolar fragmentation (23, 24). Deletion of all three SacI domain-containing 5-phosphatases is lethal; interestingly, growth and other defects in the triple mutant can be rescued by the overexpression of mammalian 5-phosphatase II (25). The yeast 5-phosphatase Inp54p contains a catalytic 5-phosphatase domain (26) but no SacI domain. Inp54p localizes to the ER membrane, and deletion of *INP54* results in increased secretion of a mammalian reporter protein bovine pancreatic trypsin inhibitor by ~2-fold relative to wild-type strains (9).

Several lines of evidence suggest that PtdIns(4,5)P_2 may play a significant role in vacuolar function. It has been proposed that PtdIns(4,5)P_2 is important for vacuolar fusion, and PtdIns(4,5)P_2 is itself synthesized during vacuolar fusion and regulates vacuole ATP-dependent priming and docking (27, 28). Although PtdIns(4,5)P_2 has not yet been identified on vacuolar membranes in intact yeast cells, *in vitro* studies revealed the recruitment of a PtdIns(4,5)P_2 biosensor to the vertices (*i.e.* the periphery of tightly apposed membranes between docked vacuoles) of vacuoles in docking reactions (28). In mammalian cells several PtdIns(4,5)P_2 lipid phosphatases, including the 5-phosphatase oculocerebrorenal protein of Lowe (OCRL) and the recently identified PtdIns(4,5)P_2 4-phosphatases, localize to lysosomal membranes, the mammalian homologue of the vacuole (29, 30). OCRL is mutated in patients with Lowe syndrome, which includes renal Fanconi syndrome, growth failure, mental retardation, cataracts, and glaucoma (29). Lysosomal hydrolase activity is elevated in plasma from Lowe syndrome patients, relative to age-matched controls (31). These studies suggest PtdIns(4,5)P_2 levels may be tightly regulated on lysosomal/vacuolar membranes.

Previous studies have shown a functional overlap between some phosphoinositide phosphatases in yeast, although not all possible phosphatase interactions have been explored (32, 33). In this study we have examined the phenotype of mutants lacking both *SAC1* and *INP54*. Inp54p hydrolyzes PtdIns(4,5)P_2 to PtdIns(4)P, whereas Sac1p hydrolyzes PtdIns(4)P to PtdIns. We investigated whether these enzymes coordinately regulate PtdIns(4,5)P_2 metabolism. We demonstrate here that although the total cellular PtdIns(4,5)P_2 levels remain unchanged in *sac1 inp54* double mutants, the spatial distribution of PtdIns(4,5)P_2 is profoundly altered, accumulating on vacuole membranes. In these double mutants, vacuolar membrane PtdIns(4,5)P_2 is derived from the plasma membrane, and its accumulation on a subset of vacuole membranes is associated with defects in vacuolar fusion. These studies reveal tight regulation of PtdIns(4,5)P_2 levels at the plasma membrane is required to regulate vacuolar fusion.

EXPERIMENTAL PROCEDURES

Materials—All restriction and DNA-modifying enzymes were obtained from Fermentas (Burlington, Canada), New England Biolabs (Beverly, MA), or Promega (Madison, WI). Oligonucleotides were obtained from GeneWorks (Adelaide, Australia). All other reagents were from Sigma or Invitrogen, unless otherwise stated. The constructs pEGFP-N1/PH-PLCδ1 and pEGFP-C1/PH-OSBP were kind gifts from Prof. Tamas Balla, NICHD, National Institutes of Health, Bethesda. GFP-PH-Num1p construct was a gift from Prof. Mark Lemmon, University of Pennsylvania, Philadelphia. Vph1p antibody was from Prof. Tom Stevens, University of Oregon, Eugene. Antibody to Clc1p was a kind gift from Prof. Gregory Payne, UCLA. MFY72 (*sac1^{ts}*) and AAY202 (*mss4^{ts}*) strains and constructs encoding *MSS4*-GFP and GFP-*STT4* were donations from Prof. Scott Emr, University of California, San Diego. Yeast strains used in this study are listed in Table 1, and plasmids are listed in Table 2.

Disruption of SAC1 and/or INP54—Deletion of *SAC1* or *INP54* from the SEY6210 strain was as described previously (9, 15). Double null *sac1 inp54* and *fig4 inp54* mutants and *sac1^{ts}* Δ*inp54* mutants were created by replacing *INP54* in the Δ*sac1*, Δ*fig4* (ResGen/Invitrogen) or MFY72 strains, respectively, with a *LEU2* cassette as described previously (9). This resulted in the deletion of a segment of chr XV from coordinates 206,284–204,565, which spans the whole open reading frame of *INP54* from nucleotides 1 to 1155, 400 bp upstream of the start codon and 166 bp downstream of the stop codon. The triple mutant *mss4^{ts}* Δ*sac1* Δ*inp54* was generated by replacing *SAC1* with a *TRP1* cassette and *INP54* with a *URA3* cassette in the *mss4^{ts}* (AAY202) strain. The *TRP1* sequence was amplified from pRS424 with the primers 5′-atgacaggtccaatagtgtacgttcaaaatgcggacggtatcttcttcaagcttgctatgtctgttattaatttcag-3′ and 5′-ttaatctcttttttaaaggatccggcttggaaaatttaggactgtgcggtatttcacaccg-3′. The PCR product was transformed into *mss4^{ts}* strains resulting in the deletion of *SAC1* from nucleotides 58 to 1830 or chr XI coordinates 34,601–36,373, creating a *mss4^{ts}* Δ*sac1* strain. *INP54*, including 1602 bp upstream of the start codon and 714 bp downstream of the stop codon, was amplified from SEY6210 genomic DNA using the primers 5′-ggctcgagttaaaacgtaagggatatgct-3′ and 5′-gcggccgctgtcgatgtactttatgt-3′ and ligated into an XhoI-NotI-digested pBIIKS(+) to generate pBINP54.

TABLE 1
Yeast strains used in this study

Strain	Genotype	Source
SEY6210	*MATα ura3-52 leu2-3, 112 his3-Δ200 trp-Δ901 lys2-801 suc2-Δ9*	63
Δ*inp54*	SEY6210, *inp54*::*LEU2*	This study
Δ*sac1* (ATY202)	SEY6210, *sac1*::*TRP1*	15
Δ*sac1* Δ*inp54*	SEY6210, *sac1*::*TRP1, inp54*::*LEU2*	This study
sac1^{ts} (MFY72)	SEY6210, *sac1*::*TRP1*, carrying pRS416*sac1^{ts}-23*	41
sac1^{ts} Δ*inp54*	MFY72, *inp54*::*LEU2*	This study
mss4^{ts} (AAY202)	SEY6210, *mss4*::*HIS3MX*, carrying YCplac111-*mss4^{ts}-102*	33
mss4^{ts} Δ*sac1* Δ*inp54*	AAY202, *sac1*::*TRP1, inp54*::*URA3*	This study
Δ*sac1* Δ*inp54*	BY4741 (*MATα his3-Δ1 leu2-Δ0 met15-Δ0 ura3-Δ0*), *sac1*::*KanMX, inp54*::*LEU2*	This study
Δ*fig4* Δ*inp54*	BY4741, *fig4*::*KanMX, inp54*::*LEU2*	This study
Δ*vps55*	BY4741, *vps55*::*KanMX*	ResGen
Δ*vps27*	BY4741, *vps27*::*KanMX*	ResGen
Δ*apm3*	BY4741, *apm3*::*KanMX*	ResGen

TABLE 2
List of plasmids used in this study

Plasmid	Description	Source
GFP-PH-*NUM1*	2μ *URA3* vector expressing GFP at the N terminus of PH-*NUM1*	44
pPS1303	2μ *URA3* vector expressing GFP under a *GAL* promoter	64
pPGK1303	pPS1303 with the *GAL* promoter replaced by a PGK promoter	This study
pPGK1303/2xPH-PLCδ1	2xPH-PLCδ1-GFP for localization of PtdIns(4,5)P_2	This study
pPGK1303/PH-OSBP	PH-OSBP-GFP for localization of PtdIns(4)P	This study
pPGK1303/*SEC14*	*SEC14*-GFP	This study
pPGK-Lys2/2xPH-PLCδ1	*LYS2* plasmid for localization of PtdIns(4,5)P_2 in *sac1^{ts}* Δ*inp54* and *mss4^{ts}* Δ*sac1* Δ*inp54* mutants	This study
pRS416-GFP/*PIK1*	*CEN URA3* plasmid expressing Pik1p-GFP under native promoter	This study
pRS426/GFP-*STT4*	2μ *URA3* plasmid expressing GFP-Stt4p under native promoter	S. Emr
pRS426/*MSS4*-GFP	2μ *URA3* plasmid expressing Mss4p-GFP under native promoter	S. Emr
pBINP54URA	For generation of *mss4^{ts}* Δ*sac1* Δ*inp54* strains	This study
pPGK423/HA-*INP54*	2μ *HIS3* plasmid expressing HA-Inp54p under the PGK promoter	This study

URA3, including its promoter, was amplified from pRS426 using the primers 5′-gactagtcgcgcgtttcggtgatgac-3′ and 5′-catgcatttacttataatacag-3′ and cloned into PstI-SpeI-digested pBINP54 to generate pBINP54URA. The *URA3* cassette flanked by the sequence upstream and downstream of *INP54* was recovered from pBINP54URA by XhoI-NotI digestion, and subsequently transformed into *mss4^{ts}* Δ*sac1* strain resulting in the deletion of *INP54*, including 400 bp upstream and 166 bp downstream of the open reading frame, creating a *mss4^{ts}* Δ*sac1* Δ*inp54* strain. Disruption of each gene was confirmed by PCR with the use of two unique sets of primers.

Yeast Immunofluorescence—For the detection of Vph1p, Pep12p, and Clc1p, yeast cells were fixed, spheroplasted, and stained as described previously (9). Anti-Vph1p and anti-Pep12p (Molecular Probes) were detected with anti-mouse Alexa-594 (Molecular Probes) and anti-Clc1p with anti-rabbit Alexa-594 (Molecular Probes). All other observations of GFP-tagged proteins were performed in live yeast cells. Fixed or live cells were placed on poly-L-lysine (2 mg/ml)-coated glass slides, and coverslips were mounted with SlowFade (Molecular Probes).

Confocal Microscopy—Yeast cells were visualized and analyzed using either an Olympus Fluoview confocal microscope or a Leica TCS NT confocal microscope, with green fluorescence collected in channel 1 (488 nm excitation, 530 ± 30 nm emission) and red fluorescence in channel 2 (568 nm excitation, LPS90 nm). Images presented in the figures show either cells in a single field or from several different fields.

Vacuole Labeling—Yeast cells were grown to mid-log phase and metabolically labeled with 20 μM FM4-64 (Sigma) for 15 min at 28 °C in YPD (34), chased in fresh YPD without FM4-64 for 30–120 min as indicated, and viewed by confocal microscopy. For analysis of endocytosis (Fig. 5), cells were labeled with 2 μM FM4-64 and viewed by confocal microscopy at the indicated time points. For CMAC-Arg labeling, *sac1^{ts}* Δ*inp54* cells were incubated with 10 μM CMAC-Arg dye (Molecular Probes) for 4 h at 28 °C, shifted to 38 °C, further incubated for 2 h, and analyzed by confocal microscopy. To assay vacuolar fragmentation or fusion, yeast cells were grown in standard YPD medium, labeled with FM4-64 for 1 h, and then shifted to YPD + 0.4 M NaCl or H_2O, respectively, for 30 min. All incubation steps were performed at 28 °C, except for *sac1^{ts}* Δ*inp54* cells that were incubated at 38 °C. Approximately 400 cells from three separate experiments were scored for vacuolar fragmentation, expressed as a percentage of the total cell population, and the mean ± S.E. was determined.

Analysis of Vacuole Function—YPD agar, pH 8.0, was prepared as described (35). Exponentially growing yeast cells were spotted onto agar plates in 10-fold serial dilutions, starting from a cell density of 10^7 cells/ml. To visualize acidified compartments, yeast cells were incubated with 0.2 mM quinacrine (Sigma) in YPD, pH 8.0, for 5 min at room temperature, as described previously (36).

Inhibition of Endocytosis—To block endocytosis, *sac1^{ts}* Δ*inp54* cells expressing 2xPH-PLC-GFP were incubated with 33 μg/ml latrunculin A (Molecular Probes) at 28 °C for 1 h, shifted to 38 °C for 1–2 h, and labeled with 20 μM FM4-64 or 10 μM CMAC-Arg (Molecular Probes).

Subcellular Localization of PtdIns(4)P and PtdIns(4,5)P_2—PH-OSBP was amplified from pEGFP-C1/PH-OSBP using the primers 5′-ggatccaaacaatgggctcggctcgagagggc-3′ and 5′-ggatccctgccagcatcttcacagc-3′, and the resulting PCR product was cloned into the BglII site of pPGK1303. 2xPH-PLCδ1 was amplified from pEGFP-N1/PH-PLCδ1 using two different sets

TABLE 3
Total cellular phosphoinositide levels

Strains	Phosphoinositides (% total [^{14}C]PtdIns ± S.E.)[a]			
	PtdIns(3)P	PtdIns(4)P	PtdIns(3,5)P$_2$	PtdIns(4,5)P$_2$
Wild-type	2.63 ± 0.32	2.43 ± 0.12	0.43 ± 0.03	1.23 ± 0.07
Δ*sac1*	5.27 ± 0.35	23.43 ± 0.98	0.73 ± 0.09	1.0 ± 0.11
Δ*sac1* Δ*inp54*	5.53 ± 0.29	25.07 ± 1.87	0.93 ± 0.09	1.2 ± 0.21
Δ*sac1* + 2μ *INP54*	5.93 ± 0.12	24.93 ± 1.18	0.97 ± 0.07	1.13 ± 0.09

[a] Data were collected from three independent experiments, and the mean ± S.E. was determined.

of primers. The first set incorporated a BamHI site at the 5′ end (5′-ggatccaaacaatggactcgggccgggac-3′) and an EcoRI site at the 3′ end (5′-gaattccttcaggaagttctg-cag-3′), and the second set incorporated an EcoRI site at the 5′ end (5′-gaattcatggactcgggccgggac-3′) and an XhoI site at the 3′ end (5′-ctcgagacttcaggaagttctgcag-3′). The two resulting PCR products were ligated together into BglII-XhoI-digested pPGK1303, and the two PH-PLCδ1 fragments simultaneously ligated via their EcoRI ends, generating two PH-PLC domains in tandem (Table 2). For expression in *sac1^{ts}* Δ*inp54* and *mss4^{ts}* Δ*sac1* Δ*inp54* strains, 2xPH-PLC-GFPδ1 was cloned in pPGK-Lys2 vector (Table 2). These constructs were subsequently transformed into yeast cells, and expression of GFP-tagged PH-OSBP, PH-PLCδ1, or PH-Num1p was analyzed live from mid-log phase cultures by confocal microscopy. Δ*sac1* Δ*inp54* and *sac1^{ts}* Δ*inp54* cells showing 2xPH-PLC-GFP on the vacuole were scored as a percentage of the total cell population, and mean ± S.E. was determined. The proportion of vacuoles expressing 2xPH-PLC-GFP on their membranes relative to the total vacuole number per cell was determined the same way. Data were collected from four independent experiments with at least 400 cells counted.

Expression of Sec14p-GFP and Pik1p-GFP—The full 912-bp *SEC14* coding sequence without the stop codon (chr XIII coordinates 424,988–426,055) was amplified by PCR from the genomic DNA of SEY6210 strain using the primers 5′-agatctatggttacacaacaagaaaaggaattttta-3′ and 5′-agatctctttcatcgaaaaggcttccgg-3′, incorporating a BglII site at each end. The resulting product was cloned into the BglII site of pPGK1303 (Table 2). The full 3198-bp *PIK1* sequence without the stop codon and 1000 bp of upstream sequence (chr XIV coordinates 140,877–144,074) was amplified by PCR using the primers 5′-ggatcctgttccatatctcggtgttgtttg-3′ and 5′-ggatcccgctatatatacctgtgtaataag-3′, incorporating a BamHI site at each end. The product was cloned in the BamHI site of pRS416-GFP (Table 2).

Analysis of CPY and General Secretion—Metabolic labeling of CPY was performed by labeling cells with 25 μCi of Easy Tag Trans^{35}S (Amersham Biosciences) per A_{600} unit at 25 °C for 5 min, followed by chasing in the presence of excess methionine and cysteine for the indicated time periods as described previously (37). CPY was immunoprecipitated using a polyclonal CPY antibody and separated on 8% SDS-PAGE, followed by fluororadiography. CPY secretion was detected using a colony immunoblot assay as described by Roberts *et al.* (36). The general secretion assay was performed as described previously (38). Following a 5-min Easy Tag Trans^{35}S labeling and a 30-min chase, NaF and NaN_3 were added to the cells to a final concentration of 20 mM each. The cell suspension was centrifuged to collect the medium fraction. Cold trichloroacetic acid was added to a final concentration of 10% to the medium fraction and incubated on ice for 30 min. Following centrifugation, the protein pellet was washed twice with acetone and sonicated in the presence of 2× Laemmli buffer and boiled, and 1 A_{600} unit was analyzed on 10% SDS-PAGE. General protein secretion was detected by fluororadiography.

Analysis of Steady-state Levels of ALP—Extraction of ALP from yeast cells was performed as described previously (39). ALP was detected using a monoclonal ALP antibody (Molecular Probes).

Analysis of Total Cellular Phosphoinositides by HPLC—[^{14}C]Inositol labeling of yeast, extraction and deacylation of lipids, and HPLC techniques were performed as described previously (15). Data were collected from three independent experiments, and the mean ± S.E. was determined.

RESULTS

Total Cellular Levels of PtdIns(4,5)P$_2$ Are Unaltered in Δ*sac1* Δ*inp54 Mutants*—Inp54p and Sac1p may act sequentially to regulate PtdIns(4,5)P$_2$ and PtdIns(4)P levels, respectively, on specific subcellular membranes. To investigate this hypothesis we generated *sac1 inp54* double null mutants (Δ*sac1* Δ*inp54*) in the SEY6210 strain background. The total cellular phosphoinositide levels were determined in null mutant yeast strains by labeling cells to equilibrium with [^{14}C]inositol. A dramatic increase in PtdIns(4)P levels was noted in Δ*sac1* cells (Table 3) (10), but all phosphoinositides, including PtdIns(4)P and PtdIns(4,5)P$_2$, were normal in Δ*inp54* mutants (not shown). PtdIns(4)P levels were increased in Δ*sac1* Δ*inp54* mutants similar to Δ*sac1* mutants. PtdIns(4)P levels in Δ*sac1* mutants were also not significantly altered by Inp54p overexpression. PtdIns(3)P and PtdIns(3,5)P$_2$ levels were increased in Δ*sac1* compared with wild-type cells, but no further significant alteration was detected in Δ*sac1* Δ*inp54* mutants or when Inp54p was overexpressed in Δ*sac1* strains (Table 3). PtdIns(4,5)P$_2$ levels have been reported to decrease 4–5-fold in Δ*sac1* cells in some studies (40, 41), whereas in three other studies (10, 15, 19) and as shown here no significant alteration in the levels of PtdIns(4,5)P$_2$ in Δ*sac1* cells was observed (Table 3). These apparent discrepancies may relate to differences in the yeast strain and/or technical distinctions in the duration and/or methods of metabolic labeling. Overexpression of Inp54p in Δ*sac1* mutants did not alter PtdIns(4,5)P$_2$ levels, relative to wild-type, Δ*sac1,* or Δ*sac1* Δ*inp54* strains. Therefore, Inp54p does not regulate PtdIns(4)P or PtdIns(4,5)P$_2$ cellular levels or interact with Sac1p to control the total cellular levels of these phosphoinositides.

PtdIns(4,5)P$_2$ Accumulates on Vacuolar Membranes upon Loss of Sac1p and Inp54p—When isolated vacuoles were labeled with a PtdIns(4,5)P$_2$ biosensor and stimulated to

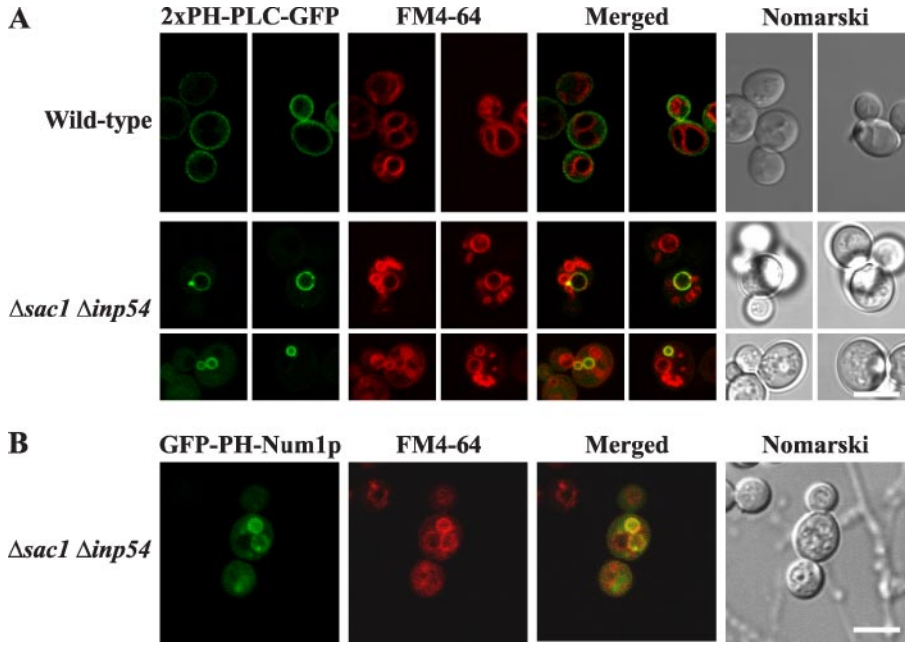

FIGURE 1. **PtdIns(4,5)P_2 accumulates on intracellular membranes upon loss of Sac1p and Inp54p.** Yeast were transformed with plasmids encoding either 2xPH-PLC-GFP (*A*) or GFP-PH-Num1p (*B*). Live samples were stained with FM4-64 for 15 min and chased for 1 h at 28 °C, except for Δ*sac1* Δ*inp54* cells that were chased for 2 h and analyzed by confocal microscopy. *Bar* = 5 μm.

undergo docking *in vitro*, PtdIns(4,5)P_2 was shown to be targeted to docking sites at vacuole vertices (28). However, in intact yeast and mammalian cells PtdIns(4,5)P_2 is detected predominantly at the plasma membrane (33, 42, 43), which is surprising given *in vitro* studies suggest PtdIns(4,5)P_2 may regulate vacuolar fusion (27, 28). To examine the spatial distribution of PtdIns(4,5)P_2 in intact yeast, we determined the localization of the PH domains of mammalian PLCδ1 and the yeast protein Num1p, which both bind PtdIns(4,5)P_2 with high affinity and specificity at the plasma membrane acting as PtdIns(4,5)P_2 biosensors (33, 42, 44). In both wild-type (Fig. 1*A*) and *inp54* null mutant (not shown) strains, 2xPH-PLC-GFP localized intensely at the plasma membrane, with little cytosolic distribution. This suggests that the 5-phosphatases Inp51-3p may compensate for the loss of Inp54p in controlling the subcellular PtdIns(4,5)P_2 distribution. In contrast, 2xPH-PLC-GFP fluorescence was redistributed to the cytoplasm in Δ*sac1* mutants, and little plasma membrane localization was detected (not shown), suggesting a decrease in PtdIns(4,5)P_2 levels at this site as reported (44). Strikingly, in Δ*sac1* Δ*inp54* mutants the PtdIns(4,5)P_2 biosensor was not detected at the plasma membrane, rather fluorescence was either diffusely cytoplasmic and/or was intensely concentrated in "ring-like" structures (Fig. 1*A*). Approximately 400 cells from four independent experiments were scored for 2x-PH-PLC-GFP distribution revealing that ~26 ± 3.0% (S.E.) of the double null mutant cell population exhibited PtdIns(4,5)P_2 biosensor vesicular accumulation with some cytosolic fluorescence, whereas the remaining cells showed only diffuse cytosolic fluorescence (see supplemental Fig. 1 for wide-field image), consistent with decreased plasma membrane PtdIns(4,5)P_2. The percentage of cells exhibiting vacuolar accumulation of the biosensor may have been underestimated because cytosolic fluorescence may obscure faint vesicular accumulation of the biosensor as the fluorescence signal to noise ratio is low in cells expressing the biosensor at low to moderate levels. Vesicular fluorescence was not observed in the wild-type or any single null mutant. The distribution of the PtdIns(4,5)P_2-specific biosensor GFP-PH-Num1p in all strains, including wild-type, Δ*inp54*, Δ*sac1,* and Δ*sac1* Δ*inp54* (Fig. 1*B*, wild-type and single mutants not shown), was the same as that shown with 2xPH-PLC-GFP (Fig. 1*A*). Specifically the PtdIns(4,5)P_2 biosensor co-localized with FM4-64 staining of intracellular membranes in Δ*sac1* Δ*inp54* mutants. These results suggest PtdIns(4,5)P_2 decreases at the plasma membrane in Δ*sac1* Δ*inp54* mutants, associated with accumulation of PtdIns(4,5)P_2 on intracellular membranes.

We characterized PtdIns(4,5)P_2-positive vesicles by co-localization with membrane markers. In Δ*sac1* Δ*inp54* mutants vesicular 2xPH-PLC-GFP fluorescence co-localized with FM4-64 staining of vacuolar membranes (Fig. 1*A*). In addition, FM4-64 staining revealed a fragmented vacuolar morphology in these double mutants, comprising a single large vacuole surrounded by multiple smaller vacuoles (see below). However, not all fragmented vacuoles exhibited PtdIns(4,5)P_2 biosensor fluorescence, and an average of 1.2 ± 0.1 vacuoles per 4.9 ± 0.6 total vacuoles within an individual cell (of 400 cells scored) exhibited 2xPH-PLC-GFP fluorescence. Deletion of *SAC1* and *INP54* in another yeast strain (BY4741) resulted in vacuolar fragmentation similar to that observed in the SEY6210 strain, and was associated with 2xPH-PLC-GFP localization to vacuole membranes (not shown).

To ensure that PtdIns(4,5)P_2 accumulation on the vacuole was not a secondary phenotype arising from two deletion mutations, we employed the use of a *sac1*^{ts} mutant, in which *INP54* was deleted. Yeast cells were grown at the permissive temperature to early log phase and then shifted to 38 °C for 1–2 h. At the permissive temperature, the PtdIns(4,5)P_2 biosensor localized to the plasma membrane in *sac1*^{ts} Δ*inp54* cells (Fig. 2*A*, see supplemental Fig. 1 for wild-field image); however, after a 1-h incubation at 38 °C, the intensity of the PtdIns(4,5)P_2 biosensor at the plasma membrane decreased significantly and instead was concentrated on intracellular vesicles that overlapped with FM4-64 labeling of endocytic intermediates (*arrows*) and the vacuole (*arrowheads*), respectively (Fig. 2*A*). By 2 h the PtdIns(4,5)P_2 biosensor exhibited no localization to endocytic intermediates and only co-localized with fragmented vacuoles (Fig. 2*A*, see supplemental Fig. 1 for wide-field image). Vacuolar fragmentation was noted only at the nonpermissive temperature.

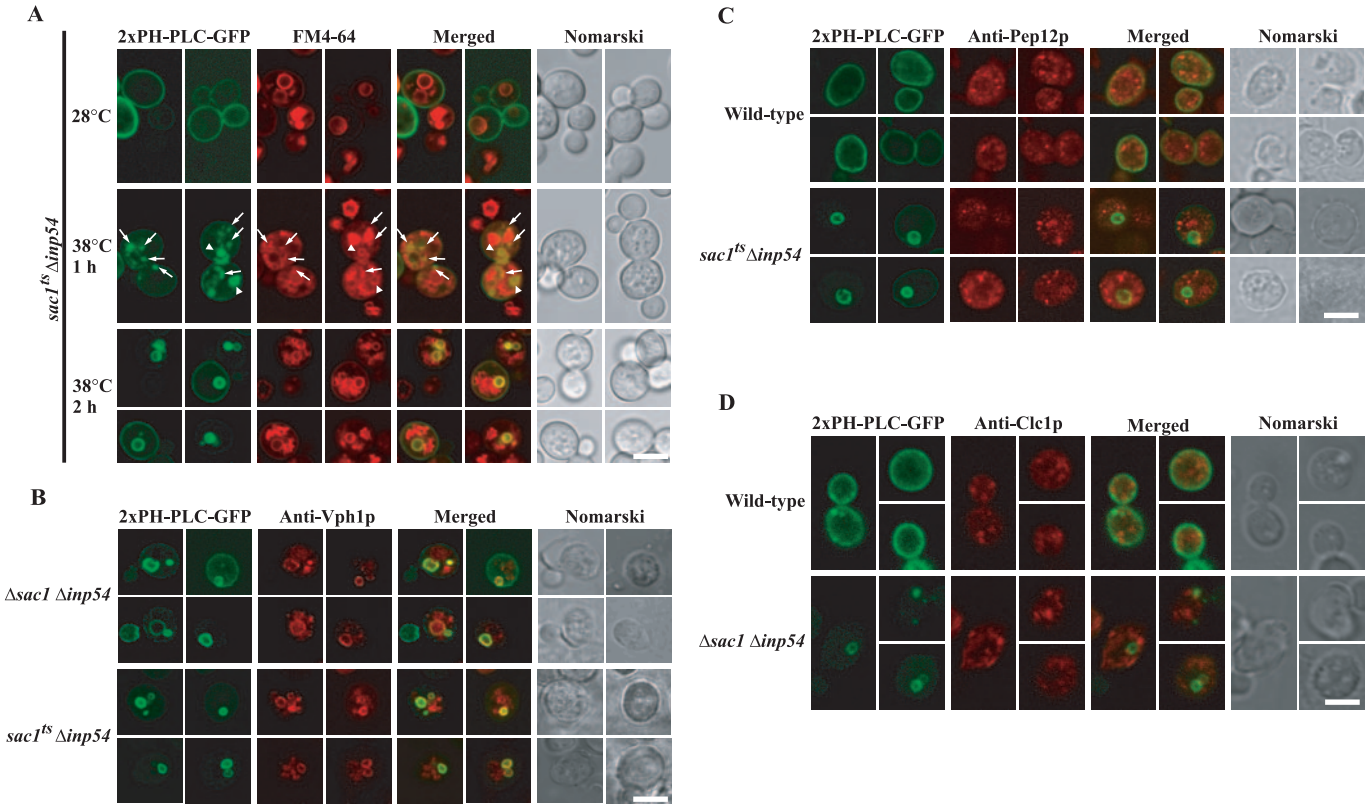

FIGURE 2. **PtdIns(4,5)P$_2$-positive vesicles co-localize with vacuolar markers.** *A, sac1^{ts} Δinp54* cells expressing 2xPH-PLC-GFP were grown at 28 °C and then shifted to 38 °C for either 1 or 2 h. Cells were co-labeled with FM4-64 to visualize intermediate endocytic structures (*arrows*) and the vacuoles (*arrowheads*). *B, Δsac1 Δinp54* or *sac1^{ts} Δinp54* cells expressing 2xPH-PLC-GFP were stained with an antibody directed against the 100-kDa subunit of the vacuolar ATPase (Vph1p). Co-localization appears *yellow* in merged images. *C,* wild-type and *sac1^{ts} Δinp54* cells expressing 2x-PH-PLC-GFP were stained with antibodies to the late endosomal marker Pep12p. *sac1^{ts} Δinp54* cells were preincubated at 38 °C for 2 h before staining. *D,* wild-type and *Δsac1 Δinp54* cells expressing 2xPH-PLC-GFP were stained with a Clc1p antibody, which binds the light chain of clathrin. *Bar* = 5 μm. Images presented are from multiple fields.

We also examined whether *Δsac1 Δinp54* inactivation regulated the spatial distribution of PtdIns(4)P, the product of 5-phosphatase hydrolysis of PtdIns(4,5)P$_2$. The localization of PtdIns(4)P was determined using the PH domain of oxysterol-binding protein (PH-OSBP) a bioprobe for PtdIns(4)P (42). In wild-type and *Δinp54* cells, PH-OSBP-GFP localized to punctate Golgi structures (supplemental Fig. 2). Despite the high levels of PtdIns(4)P in the *Δsac1* and *Δsac1Δinp54* mutants, PH-OSBP Golgi fluorescence was unchanged (supplemental Fig. 2). In additional control studies, we utilized the FYVE domain of early endosomal antigen 1 (EEA1) tagged to GFP to investigate the subcellular distribution of PtdIns(3)P, a phosphoinositide implicated in vacuolar trafficking (45). FYVE-EEA1-GFP localized to punctate endosomal structures in wild-type and all mutant strains (not shown). Therefore, in *Δsac1Δinp54* mutants only the spatial distribution of PtdIns(4,5)P$_2$ is significantly altered.

To confirm vacuolar PtdIns(4,5)P$_2$ localization, 2xPH-PLC-GFP-decorated vesicles in *Δsac1 Δinp54* and *sac1^{ts} Δinp54* mutants were co-localized with Vph1p, the 100-kDa subunit of the vacuolar ATPase (V-ATPase), a vacuolar membrane marker (Fig. 2*B*). We noted consistently that FM4-64 or V-ATPase Vph1p-labeled vesicles coincided with 2xPH-PLC-GFP fluorescence. To eliminate the possibility that 2xPH-PLC-GFP-labeled vesicles/vacuoles represent abnormal endosomal compartments, *sac1^{ts} Δinp54* cells, which had been preincubated at 38 °C for 2 h, were stained with antibodies against the late endosome resident protein Pep12p. Pep12p localized to small punctate structures in the cytosol of wild-type, *sac1^{ts} Δinp54* (Fig. 2*C*), and *Δsac1 Δinp54* strains (not shown). Although some Pep12p punctate structures overlapped with GFP-2xPH-PLC staining, there was no significant co-localization with 2xPH-PLC-GFP-labeled compartments in *sac1^{ts} Δinp54* (Fig. 2*C*) and *Δsac1 Δinp54* cells (not shown) suggesting these structures are not late endosomes. These results are consistent with the contention that PtdIns(4,5)P$_2$ accumulates on vacuoles and not endosomes.

As PtdIns(4,5)P$_2$ degradation is required for uncoating of clathrin-coated vesicles (46), we investigated whether clathrin-coated vesicles accumulate/co-localize with PtdIns(4,5)P$_2$-coated membranes in *Δsac1 Δinp54* mutants by immunostaining yeast with clathrin light chain (Clc1p) antibodies. The subcellular localization of the clathrin light chain Clc1p was similar in wild-type and all mutant strains, and no accumulation of clathrin-coated vesicles or co-localization of Clc1p with 2xPH-PLC-GFP on internal membranes in *Δsac1 Δinp54* mutants was observed (Fig. 2*D*, single mutants not shown). To exclude the possibility that the mislocalization of 2xPH-PLC-GFP in *Δsac1* and *Δsac1 Δinp54* mutants results from proteolysis of the GFP fusion proteins, anti-GFP immunoblot analysis of total cell lysates derived from wild-type, *Δinp54*, *Δsac1*, or *Δsac1 Δinp54* mutants expressing 2xPH-PLC-GFP was per-

formed. Comparable expression of intact GFP fusion proteins was detected in all strains, with little proteolysis detected (not shown).

The mislocalization of PtdIns(4,5)P_2-binding 2xPH-PLC-GFP to the vacuolar membrane in the Δ*sac1* Δ*inp54* strain may result from mislocalization of the enzymes that generate PtdIns(4,5)P_2. To exclude this possibility, the intracellular localization of the PtdIns 4-kinases Stt4p and Pik1p and the PtdIns(4)P 5-kinase Mss4p was determined in the *sac1*, *inp54* single and double null mutant cells. Pik1p and Stt4p produce ~95% of the total cellular PtdIns(4)P pool and are essential lipid kinases that contribute to the substrate pool used by Mss4p to produce PtdIns(4,5)P_2 (47). Therefore, the intracellular localization of the recently identified type II PtdIns 4-kinase Lsb6p (7) was not determined. The intracellular localization of Pik1p, Mss4p (supplemental Fig. 3, single mutants not shown), and Stt4p (not shown) was the same in wild-type and all null mutant strains. The phosphatidylinositol transfer protein Sec14p transfers phosphoinositides or phosphatidylcholine between membranes, an essential step in PtdIns(4)P and PtdIns(4,5)P_2 synthesis. Sec14p localized to punctate Golgi patches in wild-type cells, Δ*inp54*, Δ*sac1*, and Δ*sac1* Δ*inp54* mutants (supplemental Fig. 3, single mutants not shown).

Fig4p like Sac1p, contains a SacI domain, and *in vitro* assays have revealed it functions as a PtdIns(3,5)P_2-specific phosphoinositide phosphatase (13). Fig4p localizes to the limiting membrane of the vacuole and plays a role in regulating the turnover of vacuolar PtdIns(3,5)P_2. Given Sac1p and Fig4p have overlapping substrate specificity, both hydrolyze PtdIns(3,5)P_2, we examined the localization of 2xPH-PLC-GFP in Δ*fig 4* Δ*inp54* mutants (BY4741 strain background). This PtdIns(4,5)P_2 biosensor localized exclusively to the plasma membrane in the double mutant strain (supplemental Fig. 4). This suggests that Sac1p regulation of PtdIns(3,5)P_2 does not contribute to maintaining the proper subcellular distribution of PtdIns(4,5)P_2.

Loss of Sac1p and Inp54p Leads to Vacuole Fusion Defects—The cumulative results from the above experiments suggest Sac1p and Inp54p phosphatases regulate the flux of plasma membrane PtdIns(4,5)P_2. In the absence of these lipid phosphatases plasma membrane PtdIns(4,5)P_2 decreases and accumulates on a subset of fragmented vacuoles. Several questions arise from these data. First, we asked whether the fragmented vacuoles in Δ*sac1* Δ*inp54* mutants indicate a vacuole fusion defect. Vacuolar fragmentation is a marker of vacuole fusion defects (48). PtdIns(4,5)P_2 is implicated in regulating vacuolar fusion, based on *in vitro* studies (27, 28); however, it has never been detected on vacuole membranes in intact cells. Given that we had shown PtdIns(4,5)P_2 on a subset of vacuole membranes, we further characterized the vacuolar fragmentation phenotype of *sac1 inp54* double mutants. Wild-type, Δ*inp54*, and Δ*sac1* strains showed normal vacuole morphology at 28 °C, whereas the vacuoles of Δ*sac1* Δ*inp54* mutants were fragmented (see Figs. 1*A* and 5 (*120 min*)). This phenotype was also evident in *sac1*^{ts} Δ*inp54* cells when incubated at the nonpermissive temperature of 38 °C (Figs. 2*A* and 5 (*120 min*)), and correlated with the accumulation of PtdIns(4,5)P_2 on some vacuolar membranes (Figs. 2*A* and 4*B*). It is possible that PtdIns(4,5)P_2 becomes trapped on a subset of vacuole membranes that only fuse with each other, because of the high PtdIns(4,5)P_2 levels, but fail to fuse with other vacuoles, leading to PtdIns(4,5)P_2 accumulation on only a subset of membranes.

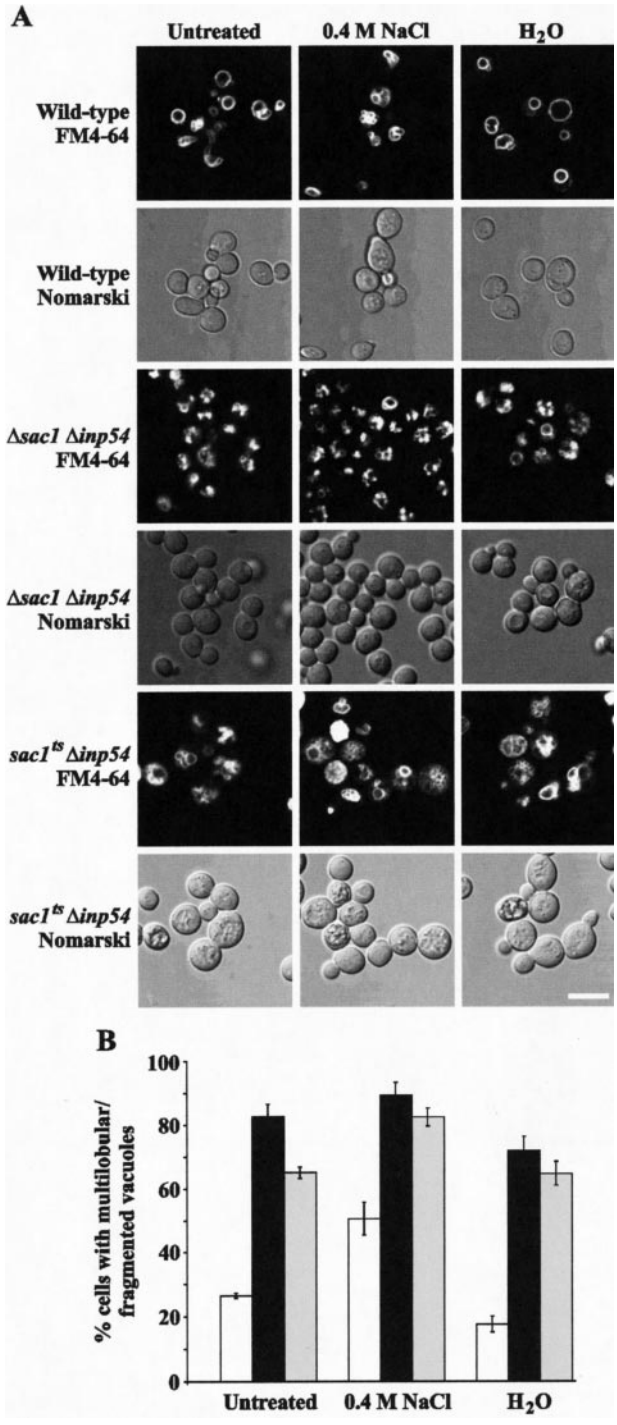

FIGURE 3. **Vacuole fusion is defective upon loss of Sac1p and Inp54p.** *A*, yeast cells were stained with 2 μM FM4-64 in standard YPD for 1 h at 28 °C and left untreated or were incubated in YPD containing 0.4 M NaCl (hyperosmotic) or H_2O (hypo-osmotic) for 30 min. *sac1*^{ts} Δ*inp54* cells were incubated at 38 °C at all stages. *Bar* = 5 μm. *B*, percentage of yeast cells showing fragmented vacuoles was determined for each strain. Approximately 400 cells from three separate experiments were scored as described under "Experimental Procedures," and the mean ± S.E. was determined. □, wild type; ■, Δ*sac1* Δ*inp54*; ▩, *sac1*^{ts} Δ*inp54*.

To analyze specifically for homotypic and/or heterotypic vacuole fusion defects in Δ*sac1* Δ*inp54* mutants, osmotic shift

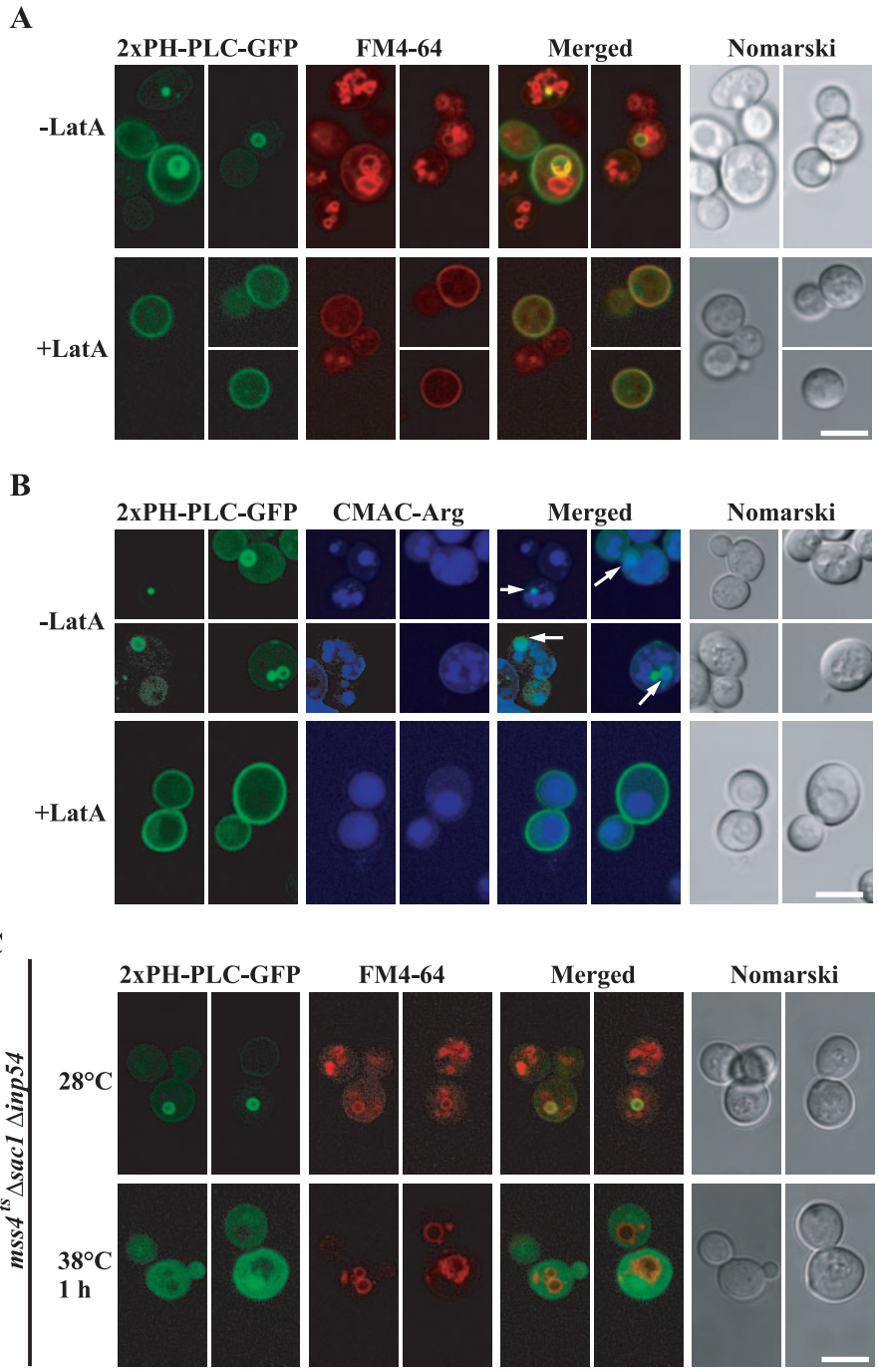

FIGURE 4. **Retention of PtdIns(4,5)P_2 at the plasma membrane rescues vacuolar fragmentation defects in *sac1 inp54* mutants.** *A*, *sac1*^{ts} Δ*inp54* cells expressing 2xPH-PLC-GFP were either left untreated or treated with 33 μg/ml latrunculin A (*LatA*) for 1 h at 28 °C, labeled with 20 μM FM4-64 for 15 min, and chased for 2 h at 38 °C. *B*, untreated *sac1*^{ts} Δ*inp54* cells were incubated with 10 μM CMAC-Arg for 4 h at 28 °C and then shifted to 38 °C for 2 h (*top panel*). *Arrows* indicate the presence of CMAC-Arg in the lumen of 2x-PH-PLC-GFP-decorated vacuoles. Latrunculin A-treated cells were incubated for 2 h at 38 °C in the presence of 10 μM CMAC-Arg (*lower panel*). *C*, *mss4*^{ts} Δ*sac1* Δ*inp54* cells expressing 2xPH-PLC-GFP were labeled with FM4-64, chased for 1 h at 28 °C (*top panel*), and then shifted to 38 °C for 1 h (*bottom panel*). *Bar* = 5 μm. Images presented are from multiple fields.

experiments were performed. Wild-type vacuoles fragment under hyperosmotic conditions and in contrast fuse in a hypo-osmotic environment (49). Wild-type, Δ*sac1* Δ*inp54*, and *sac1*^{ts} Δ*inp54* cells were grown in YPD and then incubated in either 0.4 M NaCl YPD (hyperosmotic) or water (hypo-osmotic) for 30 min. Vacuoles were scored as either nonfragmented or multi-lobed/fragmented according to the guidelines described by LaGrassa and Ungermann (49). We first examined vacuole responses to hyperosmotic treatment. Less than 30% wild-type cells showed fragmented vacuoles in untreated conditions. Upon hyperosmotic treatment, wild-type cells underwent vacuolar fragmentation with more than 50% of cells showing multiple small vacuoles (Fig. 3, *A* and *B*). >80% of Δ*sac1* Δ*inp54* and ~65% of *sac1*^{ts} Δ*inp54* cells exhibited vacuolar fragmentation in normal YPD (untreated), which increased slightly upon hyperosmotic shock (Fig. 3, *A* and *B*). We next examined for vacuolar fusion defects. Following hypo-osmotic treatment, the majority of wild-type cells exhibited nonfragmented vacuoles that had fused into one single large vacuole, so that <20% of cells exhibited fragmented vacuoles. In contrast, following hypo-osmotic treatment ~70% of Δ*sac1* Δ*inp54* and *sac1*^{ts} Δ*inp54* vacuoles remained fragmented, with no evidence of fusion (Fig. 3, *A* and *B*), indicating a general vacuolar fusion defect. Therefore, loss of the lipid phosphatases Sac1p and Inp54p leads to significant vacuolar fusion defects.

PtdIns(4,5)P_2 on Vacuole Membranes Originates from the Plasma Membrane—We next asked whether the accumulation of PtdIns(4,5)P_2 on a subset of vacuole membranes causes the observed vacuolar fusion defect. This is an important question as PtdIns(4,5)P_2 is proposed to promote vacuole fusion; however, we noted vacuole fusion defects despite evidence of increased PtdIns(4,5)P_2 on vacuole membranes. Second, we asked where the vacuolar PtdIns(4,5)P_2 comes from, given there is no evidence for a substantial vacuole pool of PtdIns(4,5)P_2 in normal yeast.

In yeast the bulk of PtdIns(4,5)P_2 is found at the plasma membrane (33, 44). To evaluate whether vacuolar PtdIns(4,5)P_2 originated from the plasma membrane, *sac1*^{ts} Δ*inp54* cells were treated with latrunculin A (1 h), which inhibits endocytosis before shifting to the restrictive temperature for 1 h (not shown) or 2 h (Fig. 4*A*). Under these conditions, FM4-64 was detected on the plasma membrane in latrunculin

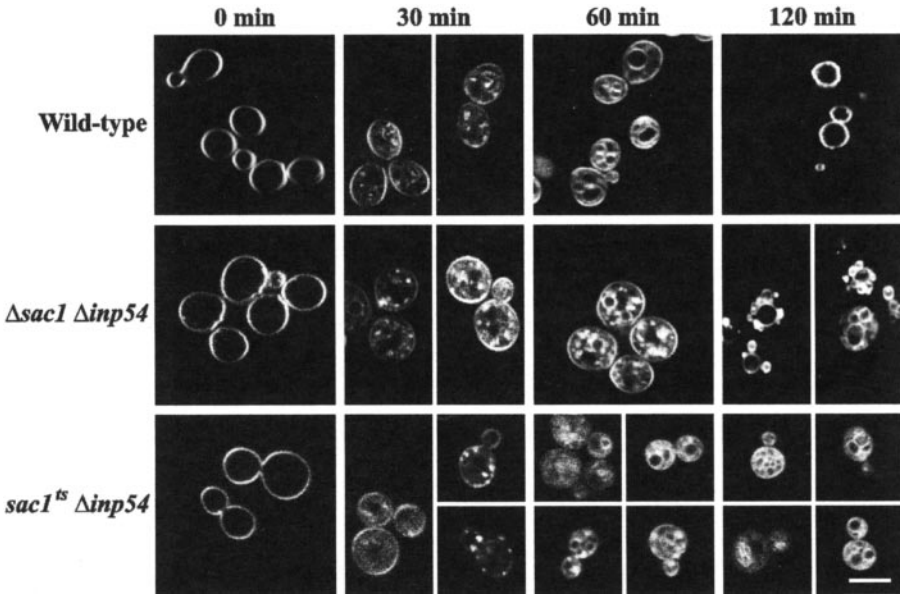

FIGURE 5. **Inactivation of Sac1p and Inp54p delays endocytosis.** Wild-type and Δ*sac1* Δ*inp54* cells were incubated with 2 μM of the endocytic/vacuolar dye FM4-64 at 28 °C, and cells were viewed live at the indicated time points by confocal microscopy. *sac1*^{ts} Δ*inp54* cells were preincubated for 1 h at 38 °C before incubation with FM4-64 at 38 °C. *Bar* = 5 μm. Images presented are from single or multiple fields.

A-treated cells indicating endocytosis was efficiently blocked (Fig. 4*A*). Significantly, the PtdIns(4,5)P_2 biosensor distribution was restricted to the plasma membrane, and no vacuolar membrane fluorescence was detected (Fig. 4*A*). Interestingly, latrunculin A treatment also rescued the vacuolar fragmentation defect in *sac1*^{ts} Δ*inp54* cells at 38 °C, as detected by the vacuole lumen stain CMAC-Arg (Fig. 4*B*, *lower panel*), consistent with the contention that PtdIns(4,5)P_2 accumulation on vacuolar membranes directly or indirectly causes the vacuolar fragmentation.

As latrunculin A also inhibits actin polymerization, which may indirectly affect vacuolar fusion, we also examined the role of plasma membrane-derived PtdIns(4,5)P_2 generated by Mss4p. *MSS4* encodes the type I phosphatidylinositol 4-phosphate 5-kinase and is the only known phosphoinositide kinase in yeast responsible for the synthesis of plasma membrane PtdIns(4,5)P_2 from PtdIns(4)P (8). Mss4p localizes to the plasma membrane, but it may also undergo phosphorylation-dependent shuttling between the plasma membrane and the nucleus (8, 50). To determine whether the vacuolar membrane PtdIns(4,5)P_2 detected in the Δ*sac1* Δ*inp54* mutants was generated by Mss4p at the plasma membrane, and next to substantiate the hypothesis that PtdIns(4,5)P_2 accumulation on vacuole membranes causes vacuolar fragmentation, a triple mutant strain containing a temperature-sensitive allele of *MSS4* was constructed, *mss4*^{ts} Δ*sac1* Δ*inp54*. Temperature-sensitive *mss4* mutants exhibit a 3-fold decrease in total cellular PtdIns(4,5)P_2 levels but no obvious vacuole fragmentation (33, 44). At the permissive temperature, 2xPH-PLC-GFP localized to a subset of fragmented vacuoles with faint plasma membrane staining in this triple mutant (Fig. 4*C*, see supplemental Fig. 5 for wide-field image). However, after 1 h at the nonpermissive temperature, both plasma membrane and vacuolar 2xPH-PLC-GFP fluorescence were significantly attenuated, and a cytosolic distribution of the PtdIns(4,5)P_2 biosensor was detected (Fig. 4*C*, see supplemental Fig. 5 for wide-field image). Significantly, under these conditions the FM4-64-labeled vacuoles appeared normal and not fragmented following inactivation of Mss4p, suggesting PtdIns(4,5)P_2 accumulation on the vacuole may trigger vacuolar fragmentation. This is concordant with our observation that latrunculin A-treated *sac1*^{ts} Δ*inp54* cells did not accumulate PtdIns(4,5)P_2 on the vacuole and displayed non-fragmented vacuoles. Collectively these studies suggest Sac1p and Inp54p control the flux of plasma membrane PtdIns(4,5)P_2 and in their absence PtdIns(4,5)P_2 may accumulate on some vacuolar membranes leading to vacuolar fragmentation.

Delayed Endocytic Trafficking to the Vacuole in sac1 inp54 Double Mutants—As we have shown evidence of significant redistribution of PtdIns(4,5)P_2 in Δ*sac1* Δ*inp54* double mutants, we examined the functional consequences. Because PtdIns(4,5)P_2 plays a role in endocytosis (1), we investigated whether endocytosis was delayed in Δ*sac1* Δ*inp54* mutants by examining the internalization of FM4-64. At 0 min FM4-64 accumulated on the cell surface in wild-type cells and both single null mutants; by 30 min the dye was packaged into endocytic vesicles, and by 60 min FM4-64 reached the vacuole (Fig. 5, single mutants not shown). Δ*sac1* Δ*inp54* and *sac1*^{ts} Δ*inp54* mutants displayed FM4-64 in endosomal compartments at 30 min at 28 and 38 °C, respectively, indicating normal internalization. However, by 60 min FM4-64 remained localized on punctate endocytic structures, although in a few cells vacuolar staining was detected. By 120 min FM4-64 had reached the partially fragmented vacuoles in Δ*sac1* Δ*inp54* and *sac1*^{ts} Δ*inp54* mutants (Fig. 5). Therefore, these double mutants exhibited evidence of delayed endocytic trafficking to the vacuole but normal internalization of endocytic vesicles from the plasma membrane. These studies suggest a role for Sac1p and Inp54p in the maintenance of vacuolar homeostasis.

sac1 and inp54 Mutants Exhibit Defects in Biosynthetic Vacuolar Trafficking—The fragmented phenotype we observed in Δ*sac1* Δ*inp54* double mutants was not unlike that exhibited by some *vps* mutants (51, 52). We therefore examined whether Sac1p and Inp54p function in directing vesicle-mediated trafficking in the endosomal system. Defects in the endocytic pathway intersect with the Golgi-to-vacuole trafficking pathway at the level of the late endosome. ER-Golgi-to-vacuole trafficking was analyzed specifically for the ability to sort and mature the vacuolar hydrolases. The transport of CPY to the vacuole was determined by metabolic labeling of cells with *trans*-[^{35}S]Cys, Met label, and chasing with excess nonradiolabeled methionine and cysteine. In wild-type and Δ*inp54* strains, CPY commenced conversion to the mature form within 5 min of chase,

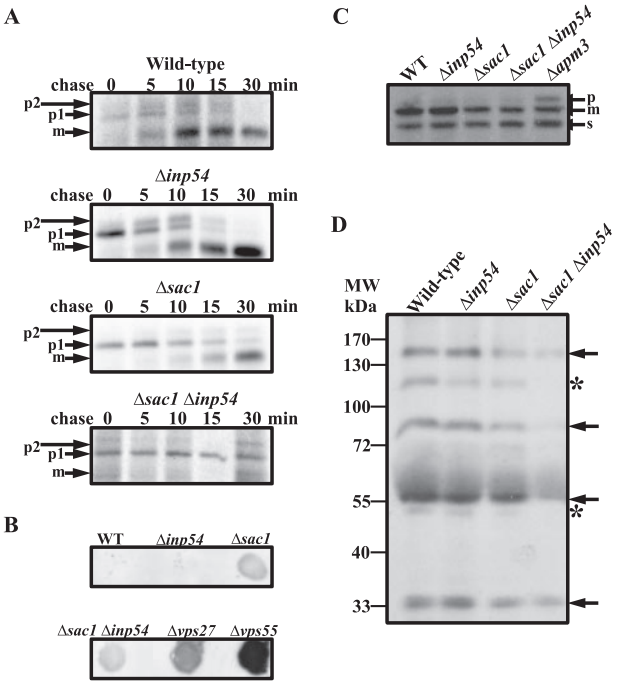

FIGURE 6. **Inp54p contributes to the function of Sac1p in regulating the classical vacuolar trafficking pathway.** *A,* yeast were metabolically labeled with *trans*-[^{35}S]Cys,Met and chased with excess nonradiolabeled methionine and cysteine at 25 °C. At each time point cell extracts were prepared, and CPY was immunoprecipitated using a CPY antibody and analyzed by SDS-PAGE and fluororadiography. *p1*, ER precursor of CPY; *p2*, Golgi precursor of CPY; *m*, vacuolar mature form of CPY. *B,* yeast cells spotted on YPD agar plates were overlaid with a nitrocellulose filter and incubated at 30 °C for 48 h, followed by immunoblotting with a CPY antibody. Δ*vps27* and Δ*vps55* strains were included as positive controls. *WT*, wild type. *C,* yeast cell extracts were immunoblotted using an ALP antibody to analyze ALP maturation. Δ*apm3* mutant cells were included as a control. *p*, precursor; *m,* mature form; *s,* soluble form. *D,* yeast cells were labeled with *trans*-[^{35}S]Cys,Met and chased with excess methionine and cysteine for 30 min. Medium was collected from each sample and protein precipitated with 10% trichloroacetic acid. An equivalent of 1 A_{600} unit for each sample was analyzed by SDS-PAGE and fluororadiography. Proteins secreted by all strains are indicated by *arrows*, and proteins not secreted by Δ*sac1* Δ*inp54* mutants are indicated by *asterisks.*

and by 10 min the prominent species was the mature CPY (Fig. 6*A*). However, Δ*sac1* mutants displayed predominantly the ER p1 form at 10 min, with little mature CPY. After 30 min of chase, mature CPY (61 kDa) was the dominant form, although the p1 form still persisted (Fig. 6*A*), as reported previously (53). This defective transport and processing of CPY appears to be a direct consequence of delayed ER to Golgi rather than Golgi-to-vacuole trafficking, as there was no significant accumulation of the Golgi p2 form (Fig. 6*A*) (53). Δ*sac1* Δ*inp54* double mutants exhibited the p1 form as the dominant species at all times, with some p2 and mature forms appearing at 30 min (Fig. 6*A*), suggesting delayed transport from the ER to a greater extent than that observed in Δ*sac1* mutants. This delay did not impact significantly on the total intracellular CPY population as steady-state Δ*sac1* Δ*inp54* mutants displayed only the mature CPY form (not shown).

CPY missorting is one of the hallmarks of *vps* mutants, characterized by misrouting of the Golgi p2 form to the secretory pathway, resulting in secretion of the precursor CPY into the extracellular medium (52). Δ*sac1* and Δ*sac1* Δ*inp54* mutants secreted CPY into the extracellular medium but to a lesser degree than the class E *vps27* mutant or the class A *vps55* mutant (Fig. 6*B*). This weak CPY secretion of Δ*sac1* has been reported previously in a large screen of the yeast genome for *vps* genes (51). The VPS-independent pathway of vacuolar trafficking, which bypasses the late endosome, was also assessed via analysis of ALP at steady-state conditions. Wild-type, Δ*inp54*, Δ*sac1*, and Δ*sac1* Δ*inp54* strains displayed the mature form of ALP and no precursor ALP, suggesting that transport to the vacuole via the ALP/AP3 pathway is unaffected in steady-state conditions; however, we cannot exclude the possibility that there is a delay in ALP processing that is undetected at steady-state levels (Fig. 6*C*). A Δ*apm3* mutant, which lacks one subunit of the AP3 adaptor complex, showed the precursor form of ALP. The soluble smaller form of ALP was also present at comparable levels in all strains.

Interestingly, several coatomer I (COPI) mutants display strong CPY maturation defects with the p1 form retained in the ER (38). These mutants also exhibit a cargo-specific secretion defect, in which some proteins are secreted normally, whereas others are blocked in secretion. To determine whether Δ*sac1* Δ*inp54* cells are compromised in COPI function, we performed a general secretion assay (38). Yeast cells were labeled with *trans*-[^{35}S]Cys,Met and chased for 30 min. Wild-type, Δ*inp54*, and Δ*sac1* cells showed a similar pattern in the secretion of various proteins to the medium; however, Δ*sac1* Δ*inp54* exhibited decreased secretion of proteins with molecular masses of ~150, 90, 55, and 33 kDa, relative to wild-type strains (Fig. 6*D, arrows*), whereas secretion of proteins with molecular masses of ~120 and 52 kDa was not apparent (Fig. 6*D, asterisks*). This suggests that inactivation of *SAC1* and *INP54* leads to impaired COPI function and thereby cargo-selective secretion defects.

Vacuolar function was assessed by analysis of growth in alkaline medium (Fig. 7*A*). Mutants defective in vacuolar acidification display increased sensitivity toward extremely acidic or alkaline medium (54). All strains grew equally well in standard YPD, but only wild-type, Δ*inp54,* and Δ*sac1* cells grew well on YPD buffered at pH 8.0 (Fig. 7*A*). Δ*sac1* Δ*inp54* mutants exhibited significant growth defects at pH 8.0. In control studies a Δ*vma2* mutant, which lacks one subunit of the V-ATPase and thus is unable to acidify the vacuole, failed to grow at pH 8.0 (Fig. 7*A*). To investigate whether the vacuole in Δ*sac1*Δ*inp54* is properly acidified, yeast cells were incubated with quinacrine, a weak base that accumulates in acidic organelles (36). Wild-type, Δ*inp54*, and Δ*sac1* cells accumulated quinacrine in the vacuole, whereas Δ*vma2* mutants did not (Fig. 7*B*). Surprisingly, Δ*sac1*Δ*inp54* mutants also accumulated quinacrine in the vacuole indicating an acidic environment (Fig. 7*B*). To test whether the vacuole in Δ*sac1*Δ*inp54* is acidified after a prolonged exposure to an alkaline environment, Δ*sac1*Δ*inp54* cells were grown in pH 8.0 YPD medium at a cell density that prevented growth on YPD plates at pH 8.0 (10^5 cells/ml). After 6 days of incubation at 30 °C, Δ*sac1*Δ*inp54* cells failed to increase in cell number, although the majority was still viable and accumulated quinacrine in the vacuole (not shown). This suggests that the vacuole in Δ*sac1*Δ*inp54* mutants is acidified sufficiently to accumulate quinacrine; however, the growth of these mutant cells at low cell density is compromised in an alkaline environment, perhaps because of subtle differences in vacuolar pH compared with wild-type cells. The presence of vacuole acidi-

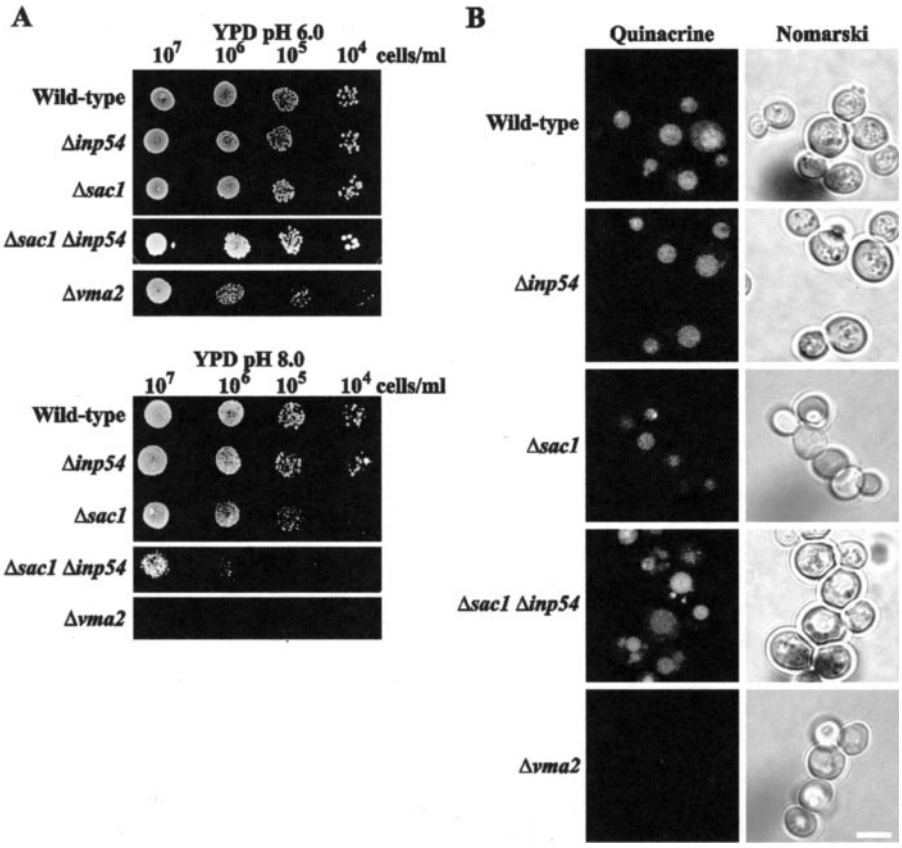

FIGURE 7. **Inp54p and Sac1p maintain normal vacuolar function.** *A,* yeast were grown in 10-fold serial dilutions starting from 10^7 cells/ml on standard YPD agar, pH 6.0, or YPD agar buffered to pH 8.0. A *vma2* mutant, which lacks one subunit of the vacuolar ATPase and failed to grow at pH 8.0, was included as a control. *B,* mid-log phase yeast cultures were incubated with 0.2 mM quinacrine in minimal medium at pH 8.0 for 5 min at room temperature. Accumulation of quinacrine indicates acidic compartments. *Bar* = 5 μm.

fication and the V-ATPase subunit Vph1p on the vacuole membrane (see Fig. 2*B*) indicates that the V-ATPase assembles and functions properly in Δ*sac1*Δ*inp54* mutants.

Thus, in summary Δ*sac1* Δ*inp54* mutants exhibit impaired vacuole fusion, delayed endocytosis, delayed ER exit of p1 CPY, cargo-selective secretion defects, and defects in vacuole function.

DISCUSSION

The results of the study described here have identified PtdIns(4,5)P_2 vacuolar membrane accumulation following inactivation of two lipid phosphatases, Sac1p and Inp54p. Evidence to support this contention was demonstrated by the vacuole membrane localization of two PtdIns(4,5)P_2-specific binding domains, which co-localized with vacuole membrane markers. We demonstrated vacuole membrane accumulation of PtdIns(4,5)P_2 in both Δ*sac1* Δ*inp54* and *sac1*^{ts} Δ*inp54* mutants, indicating this is not merely a secondary effect of these null mutations. Prior to this study, PtdIns(4,5)P_2 has not been detected previously on vacuole membranes in intact yeast cells, although *in vitro* studies reported the recruitment of PtdIns(4,5)P_2, PtdIns(3)P, ergosterol and DAG to the vertices of purified vacuoles in docking reactions (28). In mammalian cells although PtdIns(4,5)P_2 has not been detected on the mammalian homologue of the vacuole, the lysosome, several lipid phosphatases that hydrolyze PtdIns(4,5)P_2 including the OCRL 5-phosphatase, and two novel PtdIns(4,5)P_2 4-phosphatases localize to lysosomal membranes, suggesting the levels of this phosphoinositide are tightly regulated at this site (29, 30).

We propose PtdIns(4,5)P_2-vacuole membrane accumulation results from the trafficking of PtdIns(4,5)P_2-coated vesicles from the plasma membrane via the endocytic route. The results that support this hypothesis include firstly, the PtdIns(4,5)P_2 biosensor accumulated initially on endocytic structures in *sac1*^{ts} Δ*inp54* cells at the nonpermissive temperature prior to vacuole accumulation. Secondly, latrunculin A treatment which blocks endocytosis, resulted in the restriction of 2xPH-PLC-GFP fluorescence to the plasma membrane in *sac1*^{ts} Δ*inp54* mutants at the nonpermissive temperature. Thirdly, the introduction of a temperature sensitive allele of *MSS4*, which synthesizes all PtdIns(4,5)P_2 at the plasma membrane, into the Δ*sac1* Δ*inp54* strain resulted in redistribution of 2xPH-PLC-GFP fluorescence from vacuole membranes to the cytosol at the nonpermissive temperature. Therefore, PtdIns(4,5)P_2 generated by Mss4p at the plasma membrane is regulated in part by Sac1p and Inp54p, and in the absence of these phosphatases PtdIns(4,5)P_2 may accumulate on a subset of vacuole membranes.

PtdIns(4,5)P_2 Turnover Is Necessary for Proper Vacuole Fusion—PtdIns(4,5)P_2 has been proposed to regulate vacuole fusion, specifically priming and docking of vacuoles (27). However, the accumulation of PtdIns(4,5)P_2 on vacuole membranes of *sac1 inp54* double mutants was associated with vacuole fusion defects. Osmotic shift experiments revealed enhanced fragmentation in Δ*sac1* Δ*inp54* and *sac1*^{ts} Δ*inp54* strains under hyperosmotic conditions, plus a failure of the fragmented vacuoles to fuse in response to hypo-osmotic shift. Interestingly PtdIns(4,5)P_2 did not appear to accumulate on all vacuoles, this may relate to the sensitivity of the detection of PtdIns(4,5)P_2 biosensor, or alternatively, it is possible that PtdIns(4,5)P_2 accumulation on the vacuole of *sac1 inp54* mutants may result from the fusion of plasma membrane-derived PtdIns(4,5)P_2-decorated endocytic vesicles with one another, rather than with other vacuole membranes, generating a subset of PtdIns(4,5)P_2-enriched vacuoles.

An interesting question that arises from these observations is that if PtdIns(4,5)P_2 promotes vacuole fusion, why does the PtdIns(4,5)P_2-enriched vacuole not fuse with other vacuoles in the cell? It is possible that high levels of PtdIns(4,5)P_2 may change the membrane topology of the vacuole. Membrane topology depends on the lipid composition of the membrane

bilayer, and changes in lipid composition affect membrane curvature (for review see (55)). As remodeling of membrane curvature allows budding and fusion of transport vesicles, it is possible that vacuolar membrane fusion also requires this process. The high concentration of PtdIns(4,5)P_2 on some vacuole membranes in *sac1 inp54* mutants may stabilize the membrane topology to an extent that prevents further changes in membrane curvature. Alternatively, the high concentration of PtdIns(4,5)P_2 may mask other lipids that recruit other proteins which generate membrane curvature (reviewed in (56)), or proteins that facilitate vacuole fusion, *e.g.* PtdIns(3)P recruitment of Vam7p (57). As yet, it is not clear what happens to PtdIns(4,5)P_2 after vacuole priming and docking. Does it remain on the vacuole or is it hydrolyzed or sequestered away prior to fusion? Studies in mice lacking the 5-phosphatase synaptojanin 1 have revealed increased PtdIns(4,5)P_2 levels and accumulation of clathrin-coated vesicles at nerve terminals (58), indicating the importance of PtdIns(4,5)P_2 hydrolysis in vesicle uncoating, which facilitates fusion. The amount of PtdIns(4,5)P_2 on the vacuole may be critical for correct vacuolar fusion. Evidence from our studies suggests that the bulk of cellular PtdIns(4,5)P_2 has to be sequestered away from the vacuole for fusion to proceed correctly, as shown by the nonfragmented vacuoles of *sac1 inp54* mutants when PtdIns(4,5)P_2 accumulation on the vacuole is abolished by either latrunculin A treatment or inactivating Mss4p.

Docking of vacuoles, which precedes fusion, also requires vacuole acidification; this is mediated by the V-ATPase proton pump that is needed for *trans*-SNARE complex formation during docking (59). Even though the growth of Δ*sac1* Δ*inp54* mutants was compromised in alkaline medium, their vacuoles were sufficiently acidic to accumulate quinacrine. Furthermore, the presence of the V-ATPase subunit Vph1p on the vacuole membrane suggests that the V-ATPase proton pump assembles and functions properly in these mutants. Therefore, any defect in vacuole docking/fusion is more likely to be caused by PtdIns(4,5)P_2 accumulation on the vacuole, rather than from compromised acidification.

We propose that PtdIns(4,5)P_2 hydrolysis by lipid phosphatases is important for regulating vacuole fusion. Indeed, a genomic screen of yeast deletion mutants with vacuolar fragmentation suggests regulation of PtdIns(4,5)P_2 by phospholipase C is essential for vacuole fusion (48). In the same study, an *inp54* mutant was also found to display vacuolar fragmentation, in contrast to our findings that Δ*inp54* mutants have normal vacuole morphology. This may be due to strain-specific differences. Double deletions of *INP51, -52,* and *-53* resulted in fragmented vacuoles, again highlighting the importance of PtdIns(4,5)P_2 turnover in regulating vacuole fusion (23, 24).

Possible Functional Interaction of Sac1p and Inp54p in Vacuolar Function/Homeostasis—There are four distinct lipid phosphatases in yeast that hydrolyze PtdIns(4,5)P_2 forming PtdIns(4)P, Inp51-4p. In addition to their 5-phosphatase domain, Inp52p and Inp53p also contain a SacI-like catalytic domain, which functions principally to regulate the levels of PtdIns(4)P, as does Sac1p itself. It has been proposed that Inp52p and/or Inp53p can each hydrolyze PtdIns(4,5)P_2 to PtdIns(4)P by the 5-phosphatase domain and then PtdIns(4)P to PtdIns by the SacI-like domain (10). In contrast, Inp51p and Inp54p do not have a functional SacI-like domain. Although there is no reason *per se* to anticipate that Sac1p and Inp54p should functionally interact and given Inp54p is one of two yeast 5-phosphatases that does not have a functional SacI domain, it was possible that Sac1p serves this role for Inp54p. Equally possible, although not explored here, Inp51p may interact with Sac1p, as this 5-phosphatase also lacks a functional SacI domain.

A critical question to address is whether Sac1p and Inp54p functionally interact to regulate vesicular trafficking and/or vacuole fusion. The major defects noted in the *sac1 inp54* mutants were vacuolar fragmentation and fusion defects, delayed CPY sorting, a marker of ER-Golgi-to-vacuole trafficking, associated with specific cargo secretion defects, suggesting impaired coatomer I (COPI) function (38). The latter observation is consistent with recent studies that revealed members of the COPI complex functionally interact with human SAC1 (60).

Despite vacuole fusion defects, CPY and FM4-64, although delayed, and ALP can reach the vacuole in Δ*sac1* Δ*inp54* mutants. This could be explained by the different requirements for homotypic vacuole fusion and heterotypic fusion between other organelles and the vacuoles. A defect in homotypic vacuole fusion does not necessarily indicate a defect in cargo sorting to the vacuole. For example, the vacuolar v-SNARE Nyv1p is required for vacuole docking (61), which precedes vacuole-vacuole fusion, but it is not required in the biosynthetic pathways to the vacuole (62). A genomic screen of 4828 nonessential gene deletions in yeast revealed many mutants with vacuolar fragmentation but no *vps* phenotype (48), which indicates that there is an overlap as well as distinction between pathways of trafficking to the vacuole and vacuole-vacuole fusion.

In summary, this study has demonstrated the lipid phosphatases Sac1p and Inp54p regulate plasma membrane PtdIns(4,5)P_2 distribution. Although PtdIns(4,5)P_2 has been implicated in vacuolar function, this study shows that PtdIns(4,5)P_2 can accumulate on vacuole membranes in the absence of specific lipid phosphatases in intact yeast cells and is associated with vacuole fusion defects.

Acknowledgments—We thank Scott Emr, Mark Lemmon, Randy Schekman, Mike Lewis, and Peter Novick for kindly donating constructs; Gregory Payne and Tom Stevens for antibodies; Jennifer Dyson for critical reading of the manuscript; Jon Audhya, Carlos Rosado and Dalibor Mijaljica for technical advice.

REFERENCES

1. Roth, M. G. (2004) *Physiol. Rev.* **84,** 699–730
2. Hama, H., Schnieders, E. A., Thorner, J., Takemoto, J. Y., and DeWald, D. B. (1999) *J. Biol. Chem.* **274,** 34294–34300
3. Godi, A., Di Campli, A., Konstantakopoulos, A., Di Tullio, G., Alessi, D. R., Kular, G. S., Daniele, T., Marra, P., Lucocq, J. M., and De Matteis, M. A. (2004) *Nat. Cell Biol.* **6,** 393–404
4. Flanagan, C. A., Schnieders, E. A., Emerick, A. W., Kunisawa, R., Admon, A., and Thorner, J. (1993) *Science* **262,** 1444–1448
5. Yoshida, S., Ohya, Y., Goebl, M., Nakano, A., and Anraku, Y. (1994) *J. Biol. Chem.* **269,** 1166–1172
6. Audhya, A., and Emr, S. D. (2002) *Dev. Cell* **2,** 593–605
7. Han, G. S., Audhya, A., Markley, D. J., Emr, S. D., and Carman, G. M.

(2002) *J. Biol. Chem.* **277,** 47709–47718
8. Homma, K., Terui, S., Minemura, M., Qadota, H., Anraku, Y., Kanaho, Y., and Ohya, Y. (1998) *J. Biol. Chem.* **273,** 15779–15786
9. Wiradjaja, F., Ooms, L. M., Whisstock, J. C., McColl, B., Helfenbaum, L., Sambrook, J. F., Gething, M. J., and Mitchell, C. A. (2001) *J. Biol. Chem.* **276,** 7643–7653
10. Guo, S., Stolz, L. E., Lemrow, S. M., and York, J. D. (1999) *J. Biol. Chem.* **274,** 12990–12995
11. Stolz, L. E., Kuo, W. J., Longchamps, J., Sekhon, M. K., and York, J. D. (1998) *J. Biol. Chem.* **273,** 11852–11861
12. Ooms, L. M., McColl, B. K., Wiradjaja, F., Wijayaratnam, A. P., Gleeson, P., Gething, M. J., Sambrook, J., and Mitchell, C. A. (2000) *Mol. Cell. Biol.* **20,** 9376–9390
13. Rudge, S. A., Anderson, D. M., and Emr, S. D. (2004) *Mol. Biol. Cell* **15,** 24–36
14. Faulhammer, F., Konrad, G., Brankatschk, B., Tahirovic, S., Knodler, A., and Mayinger, P. (2005) *J. Cell Biol.* **168,** 185–191
15. Schorr, M., Then, A., Tahirovic, S., Hug, N., and Mayinger, P. (2001) *Curr. Biol.* **11,** 1421–1426
16. Cleves, A. E., Novick, P. J., and Bankaitis, V. A. (1989) *J. Cell Biol.* **109,** 2939–2950
17. Hughes, W. E., Pocklington, M. J., Orr, E., and Paddon, C. J. (1999) *Yeast* **15,** 1111–1124
18. Novick, P., Osmond, B. C., and Botstein, D. (1989) *Genetics* **121,** 659–674
19. Rivas, M. P., Kearns, B. G., Xie, Z., Guo, S., Sekar, M. C., Hosaka, K., Kagiwada, S., York, J. D., and Bankaitis, V. A. (1999) *Mol. Biol. Cell* **10,** 2235–2250
20. Whitters, E. A., Cleves, A. E., McGee, T. P., Skinner, H. B., and Bankaitis, V. A. (1993) *J. Cell Biol.* **122,** 79–94
21. Tahirovic, S., Schorr, M., and Mayinger, P. (2005) *Traffic* **6,** 116–130
22. Cleves, A. E., McGee, T. P., Whitters, E. A., Champion, K. M., Aitken, J. R., Dowhan, W., Goebl, M., and Bankaitis, V. A. (1991) *Cell* **64,** 789–800
23. Srinivasan, S., Seaman, M., Nemoto, Y., Daniell, L., Suchy, S. F., Emr, S., De Camilli, P., and Nussbaum, R. (1997) *Eur. J. Cell Biol.* **74,** 350–360
24. Stolz, L. E., Huynh, C. V., Thorner, J., and York, J. D. (1998) *Genetics* **148,** 1715–1729
25. O'Malley, C. J., McColl, B. K., Kong, A. M., Ellis, S. L., Wijayaratnam, A. P., Sambrook, J., and Mitchell, C. A. (2001) *Biochem. J.* **355,** 805–817
26. Raucher, D., Stauffer, T., Chen, W., Shen, K., Guo, S., York, J. D., Sheetz, M. P., and Meyer, T. (2000) *Cell* **100,** 221–228
27. Mayer, A., Scheglmann, D., Dove, S., Glatz, A., Wickner, W., and Haas, A. (2000) *Mol. Biol. Cell* **11,** 807–817
28. Fratti, R. A., Jun, Y., Merz, A. J., Margolis, N., and Wickner, W. (2004) *J. Cell Biol.* **167,** 1087–1098
29. Zhang, X., Hartz, P. A., Philip, E., Racusen, L. C., and Majerus, P. W. (1998) *J. Biol. Chem.* **273,** 1574–1582
30. Ungewickell, A., Hugge, C., Kisseleva, M., Chang, S. C., Zou, J., Feng, Y., Galyov, E. E., Wilson, M., and Majerus, P. W. (2005) *Proc. Natl. Acad. Sci. U. S. A.* **102,** 18854–18859
31. Ungewickell, A. J., and Majerus, P. W. (1999) *Proc. Natl. Acad. Sci. U. S. A.* **96,** 13342–13344
32. Parrish, W. R., Stefan, C. J., and Emr, S. D. (2004) *Mol. Biol. Cell* **15,** 3567–3579
33. Stefan, C. J., Audhya, A., and Emr, S. D. (2002) *Mol. Biol. Cell* **13,** 542–557
34. Vida, T. A., and Emr, S. D. (1995) *J. Cell Biol.* **128,** 779–792
35. Hongay, C., Jia, N., Bard, M., and Winston, F. (2002) *EMBO J.* **21,** 4114–4124
36. Roberts, C. J., Raymond, C. K., Yamashiro, C. T., and Stevens, T. H. (1991) *Methods Enzymol.* **194,** 644–661
37. Munn, A. L., Heese-Peck, A., Stevenson, B. J., Pichler, H., and Riezman, H. (1999) *Mol. Biol. Cell* **10,** 3943–3957
38. Gaynor, E. C., and Emr, S. D. (1997) *J. Cell Biol.* **136,** 789–802
39. Belgareh-Touze, N., Avaro, S., Rouille, Y., Hoflack, B., and Haguenauer-Tsapis, R. (2002) *Mol. Biol. Cell* **13,** 1694–1708
40. Hughes, W. E., Woscholski, R., Cooke, F. T., Patrick, R. S., Dove, S. K., McDonald, N. Q., and Parker, P. J. (2000) *J. Biol. Chem.* **275,** 801–808
41. Foti, M., Audhya, A., and Emr, S. D. (2001) *Mol. Biol. Cell* **12,** 2396–2411
42. Levine, T. P., and Munro, S. (2002) *Curr. Biol.* **12,** 695–704
43. Varnai, P., and Balla, T. (1998) *J. Cell Biol.* **143,** 501–510
44. Yu, J. W., Mendrola, J. M., Audhya, A., Singh, S., Keleti, D., DeWald, D. B., Murray, D., Emr, S. D., and Lemmon, M. A. (2004) *Mol. Cell* **13,** 677–688
45. Burd, C. G., and Emr, S. D. (1998) *Mol. Cell* **2,** 157–162
46. Haucke, V. (2005) *Biochem. Soc. Trans.* **33,** 1285–1289
47. Audhya, A., Foti, M., and Emr, S. D. (2000) *Mol. Biol. Cell* **11,** 2673–2689
48. Seeley, E. S., Kato, M., Margolis, N., Wickner, W., and Eitzen, G. (2002) *Mol. Biol. Cell* **13,** 782–794
49. LaGrassa, T. J., and Ungermann, C. (2005) *J. Cell Biol.* **168,** 401–414
50. Audhya, A., and Emr, S. D. (2003) *EMBO J.* **22,** 4223–4236
51. Bonangelino, C. J., Chavez, E. M., and Bonifacino, J. S. (2002) *Mol. Biol. Cell* **13,** 2486–2501
52. Raymond, C. K., Howald-Stevenson, I., Vater, C. A., Stevens, T. H., Roberts, C. J., Moore, K. E., and Howald, I. (1992) *Mol. Biol. Cell* **3,** 1389–1402
53. Kochendorfer, K. U., Then, A. R., Kearns, B. G., Bankaitis, V. A., and Mayinger, P. (1999) *EMBO J.* **18,** 1506–1515
54. Banta, L. M., Robinson, J. S., Klionsky, D. J., and Emr, S. D. (1988) *J. Cell Biol.* **107,** 1369–1383
55. McMahon, H. T., and Gallop, J. L. (2005) *Nature* **438,** 590–596
56. Zimmerberg, J., and Kozlov, M. M. (2006) *Nat. Rev. Mol. Cell Biol.* **7,** 9–19
57. Boeddinghaus, C., Merz, A. J., Laage, R., and Ungermann, C. (2002) *J. Cell Biol.* **157,** 79–89
58. Cremona, O., Di Paolo, G., Wenk, M. R., Luthi, A., Kim, W. T., Takei, K., Daniell, L., Nemoto, Y., Shears, S. B., Flavell, R. A., McCormick, D. A., and De Camilli, P. (1999) *Cell* **99,** 179–188
59. Ungermann, C., Wickner, W., and Xu, Z. (1999) *Proc. Natl. Acad. Sci. U. S. A.* **96,** 11194–11199
60. Rohde, H. M., Cheong, F. Y., Konrad, G., Paiha, K., Mayinger, P., and Boehmelt, G. (2003) *J. Biol. Chem.* **278,** 52689–52699
61. Nichols, B. J., Ungermann, C., Pelham, H. R., Wickner, W. T., and Haas, A. (1997) *Nature* **387,** 199–202
62. Fischer von Mollard, G., and Stevens, T. H. (1999) *Mol. Biol. Cell* **10,** 1719–1732
63. Wilsbach, K., and Payne, G. S. (1993) *EMBO J.* **12,** 3049–3059
64. Shen, E. C., Henry, M. F., Weiss, V. H., Valentini, S. R., Silver, P. A., and Lee, M. S. (1998) *Genes Dev.* **12,** 679–691

SUPPLEMENTARY FIGURE LEGENDS

Supplementary Figure 1. PtdIns(4,5)P_2 accumulates on intracellular membranes upon loss of Sac1p and Inp54p. Yeast cells were transformed with 2xPH-PLC-GFP plasmids and viewed live under confocal microscopy. *Δsac1 Δinp54* cells were grown at 28°C (top panel), *sac1^{ts} Δinp54* cells were grown at 28°C (middle panel), and then shifted to 38°C for 2 hours (bottom panel). Bar = 5 μm.

Supplementary Figure 2. Subcellular distribution of PtdIns(4)P in *Δsac1 Δinp54* cells. Yeast cells were transformed with a plasmid encoding PH-OSBP-GFP. Early log-phase cultures of yeast were viewed live under confocal microscopy. Bar = 5 μm.

Supplementary Figure 3. Subcellular localization of enzymes involved in PtdIns(4,5)P_2 synthesis. Wild-type and *Δsac1 Δinp54* strains were transformed with GFP-tagged *PIK1* or *MSS4* under their native promoters, or *SEC14* fused to GFP under a constitutive PGK promoter, and viewed live by confocal microscopy. Bar = 5 μm. Images presented are from single or multiple fields.

Supplementary Figure 4. Double deletion of *FIG4* and *INP54* does not affect PtdIns(4,5)P_2 subcellular distribution. *Δfig4 Δinp54* cells were transformed with plasmids encoding 2xPH-PLC-GFP. Live samples were stained with FM4-64 for 15 mins and chased for 1 hour at 28°C, and analyzed by confocal microscopy. Bar = 5 μm.

Supplementary Figure 5. Retention of PtdIns(4,5)P_2 at the plasma membrane rescues vacuolar fragmentation defects in *Δsac1 Δinp54* mutants. *mss4^{ts} Δsac1 Δinp54* cells expressing 2xPH-PLC-GFP were grown at 28°C (top panel), and then shifted to 38°C for 1 hour (bottom panel). Bar = 5 μm.

Supplementary Figure 1

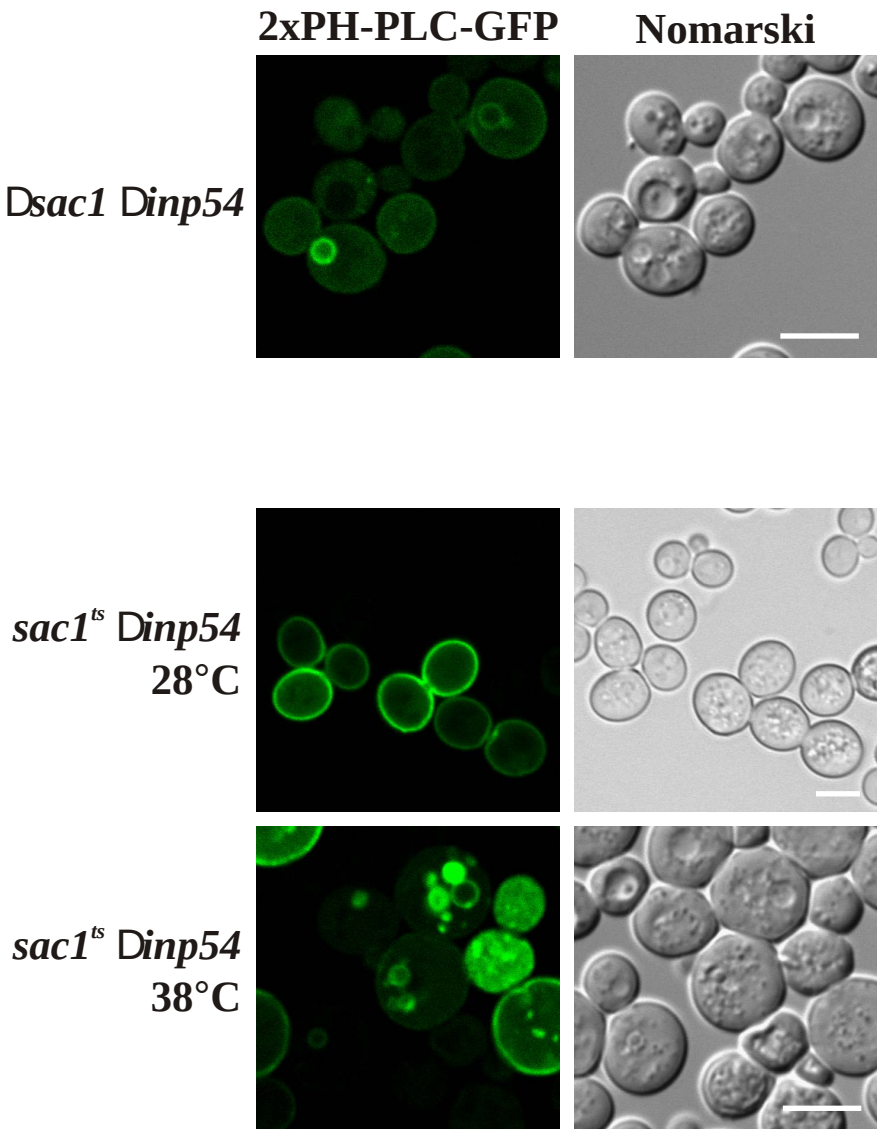

Supplementary Figure 2

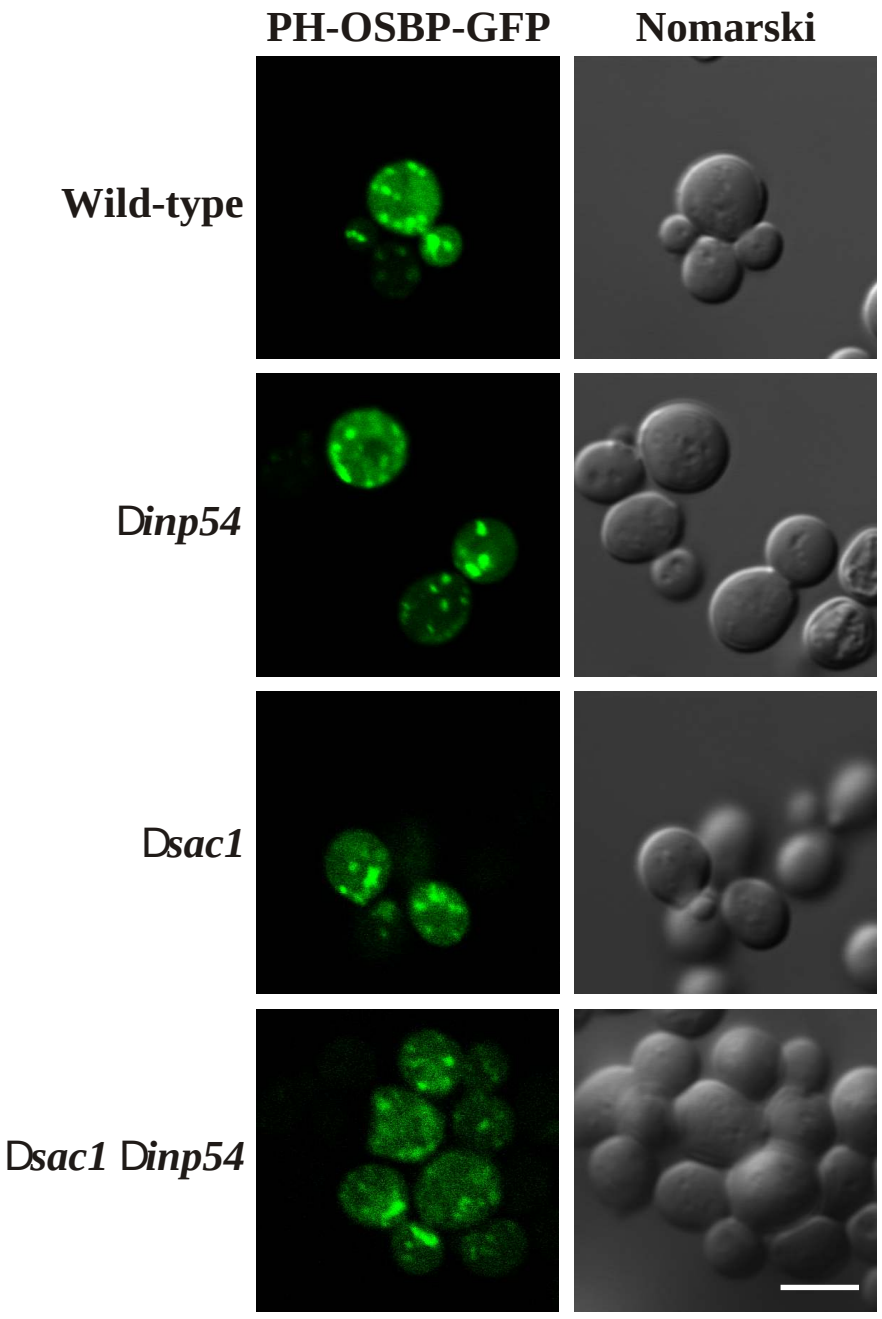

Supplementary Figure 3

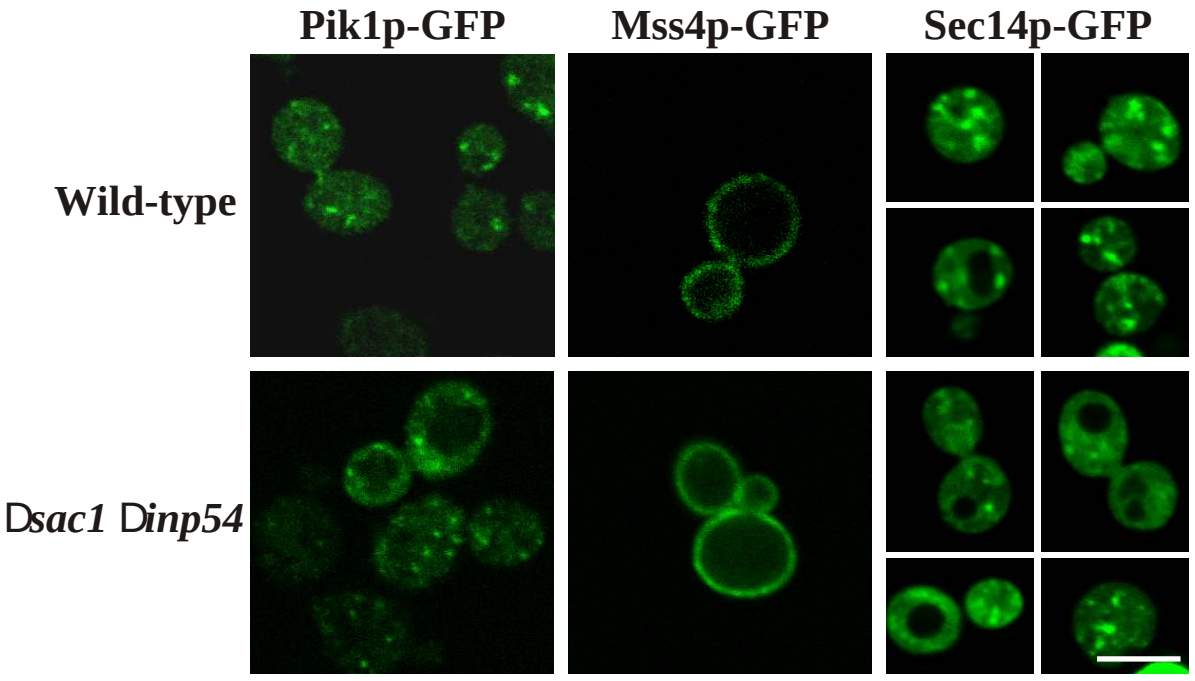

Supplementary Figure 4

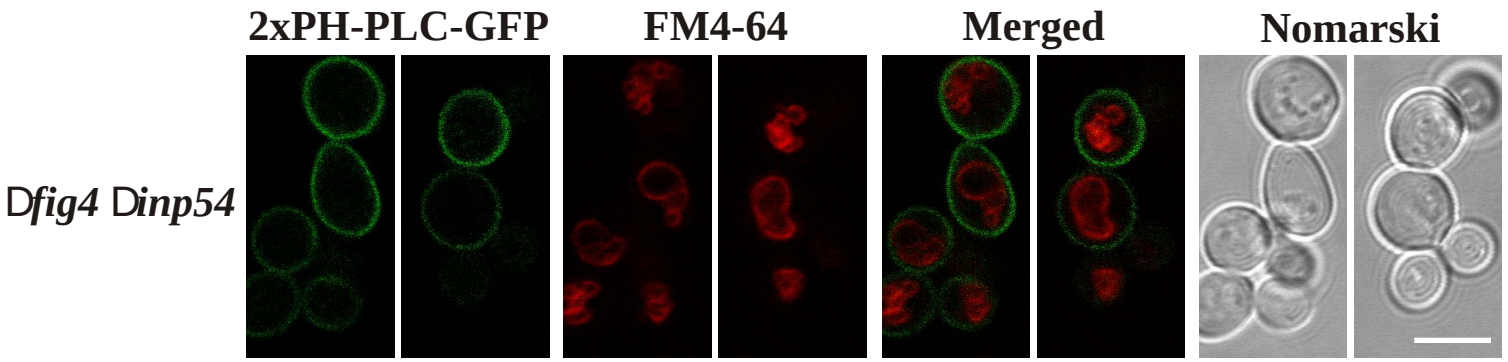

Supplementary Figure 5

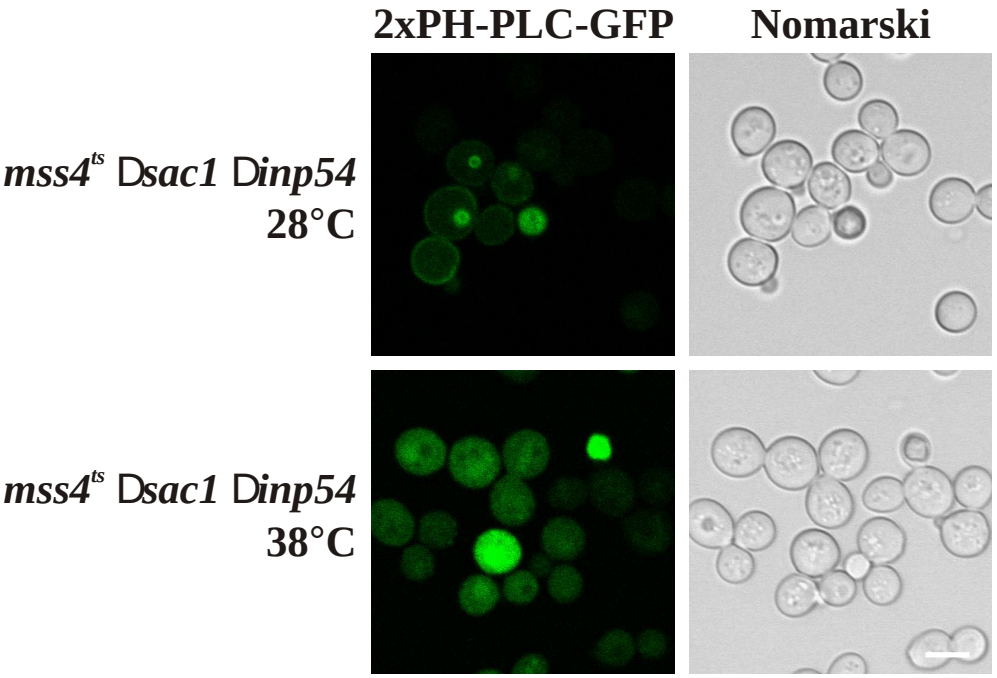

Inactivation of the Phosphoinositide Phosphatases Sac1p and Inp54p Leads to Accumulation of Phosphatidylinositol 4,5-Bisphosphate on Vacuole Membranes and Vacuolar Fusion Defects

Fenny Wiradjaja, Lisa M. Ooms, Sabina Tahirovic, Ellie Kuhne, Rodney J. Devenish, Alan L. Munn, Robert C. Piper, Peter Mayinger and Christina A. Mitchell

J. Biol. Chem. 2007, 282:16295-16307.
doi: 10.1074/jbc.M701038200 originally published online March 28, 2007
